Norwegian University of Life Sciences
Faculty of Environmental Sciences
and Natural Resource Management

Philosophiae Doctor (PhD)
Thesis 2020:30

A novel framework for coupling mesoscale and steady-state CFD models for wind resource assessment

Ny metodikk for kobling av mesoskala og stasjonære CFD modeller for vindressurskartlegging

Pablo Durán

A novel framework for coupling mesoscale and steady-state CFD models for wind resource assessment

Ny metodikk for kobling av mesoskala og stasjonære CFD modeller for vindressurskartlegging

Philosophiae Doctor (PhD) Thesis

Pablo Durán

Norwegian University of Life Sciences
Faculty of Environmental Sciences and Natural Resource Management

Ås (2020)

Thesis number 2020:30
ISSN 1894-6402
ISBN 978-82-575-1693-2

PhD Supervisors

Professor Muyiwa Samuel Adaramola
Faculty of Environmental Sciences and Natural Resource Management
Norwegian University of Life Sciences
Ås, Norway

Dr. Catherine Meissner
Wattsight AS
Oslo, Norway

Associate Professor Sukanta Basu
Faculty of Civil Engineering and Geosciences
Delft University of Technology
Delft, The Netherlands

Dr. Arne Reidar Gravdahl
WindSim AS
Tønsberg, Norway

Evaluation committee

Dr. Erik Berge
Norwegian Meteorological Institute (MET)
Oslo, Norway

Dr. Carolin Schmitt
EnBW Energie Baden-Württemberg AG
Karlsruhe, Germany

Associate Professor Nils-Otto Kitterød
Faculty of Environmental Sciences and Natural Resource Management
Norwegian University of Life Sciences
Ås, Norway

Acknowledgments

First of all, I would like to thank all my supervisors for their advice and support during my PhD. Sam, you were always encouraging, and I always left your office in a better mood. A special thanks to Catherine for her dedication during my PhD. You were key in the direction and quality of the research. I have not only learned from your technical knowledge, but you were also an example for my professional life. I am also very grateful to Sukanta. It has been a real pleasure to collaborate with you and I hope we have the chance to work together again in the future. You always had those challenging questions that pushed me to investigate further. Last, but not least, thank you Arne for your supervision and useful discussions.

I would like to thank my partner Cecilie for her unconditional support during my PhD. You always showed an honest technical interest in my work and put time and effort into reading and discussing it. I am also grateful to my colleagues at WindSim: Di, Matteo, Ricardo, Tejo and Tine. I have learned a lot with you during these 3 years and it has been a pleasure to go with you to conferences, “julebord” and courses. I would also like to thank all my colleagues at MINA who were part of my everyday life at Sørhellinga. I would like to thank in particular Denis, Franz, Kristel, Mari, Mekdes, Miguel, Nils, Ross, Ruben, Silke, Solrun, Thomas, Vilde, Yennie, Yi-kuang and Yngvild. Finally, I would like to extend my gratitude to the renewable energy group as well as to the administrative team at Sørhellinga.

Sandvika, February 2020

Pablo Durán

Summary

The estimation of the energy production of wind farms is a key factor for the development of wind energy projects. Currently, these estimations utilize only a few onsite measurement points to estimate the wind resource at the location of the wind turbines by means of a wind flow model. One of the most advanced wind flow models utilized in the wind energy industry for this purpose are the steady-state computational fluid dynamic (CFD) models. These models have proven to be successful in modelling the wind flow in complex terrain. Nevertheless, there are some limitations in their applicability at sites with complex weather patterns.

In this PhD thesis, these limitations are addressed by coupling a CFD model with a mesoscale meteorological model (MMM). MMMs are widely used for weather forecast and can reproduce the complex weather phenomena that a CFD model lacks. In this study, the framework to couple both models consists in utilizing the mesoscale simulation results to compute the boundary conditions of the CFD model. Two variants of the meso-microscale coupling approach are here studied.

The first approach consists in utilizing the average values of the mesoscale fields by wind directional sector. It is shown that this approach improves the wind estimations in complex terrain and in areas that are located at the wake of the terrain features of a site. Nevertheless, the approach presents important limitations in sites where the wind blows from few wind directions. The second approach addresses this limitation by extracting weather patterns from the mesoscale simulations by means of a fully automated clustering methodology. This classification technique is capable of extracting the predominant weather patterns and organizing them in a meaningful way. Overall, by downscaling the extracted patterns the modelling error is reduced compared with the mesoscale model. Such a methodology has a lot of potential for wind turbine wake studies as well as for forecasting solutions that utilize CFD models.

Table of Contents

List of Papers

Paper I

Meso-microscale coupling for wind resource assessment using averaged atmospheric stability conditions
Durán P, Meißner C, Rutledge K, Fonseca R, Martin-Torres J, Adaramola MS
Published in Meteorologische Zeitschrift (2019)
doi: 10.1127/metz/2019/0937

Paper II

Automated classification of simulated wind field patterns from multiphysics ensemble forecasts
Durán P, Basu S, Meißner C, Adaramola MS
Published in Wind Energy (2019)
doi: 10.1002/we.2462

Paper III

A new meso-microscale coupled modelling framework for wind resource assessment: A validation study
Durán P, Meiβner C, Casso P
Submitted to Renewable Energy

Paper IV

Wind resource assessment using a novel meso-microscale coupling framework based on two-level self-organized maps clustering: A preliminary study
Durán P
Manuscript

Chapter 1

Introduction

The goal of this section is to provide to the reader a context for the research described in this PhD thesis. Both the motivation of this research and their objectives are presented. Finally, the contents of the thesis are outlined, including the relation between the scientific articles of this thesis.

1.1 Motivation of the research

Wind energy generation has been identified by the Intergovernmental Panel on Climate Change as one of the renewable technologies with the highest mitigation potential due to its relatively low lifecycle greenhouse gas emissions and competitive costs.[1] The latter has driven a continuous increase in the total installed capacity of wind energy around the world.[2] By far, the most important factor for the profitability of a wind energy project is the total amount of energy produced,[3] which in turn depends on the available wind resource and wind farm layout. In the planning phase of a wind energy project, energy produced by wind farm is estimated through a process called wind resource assessment. The main goal of this process is to predict the windiest locations within a given area. Due to the cost, it is only possible to concurrently measure wind speed and its associated variables (such as wind direction, ambient temperature and atmospheric pressure) in a limited number of locations within a given site considered for a wind farm. Therefore, a method is required to extrapolate few measurements to other locations of interest. For this purpose, the wind industry typically uses the so-called numerical wind flow models. These models are designed to predict the spatial variation of the wind by modelling the physical behavior of the wind flow.

The wind flow models that are mostly utilized for wind resource assessment in the industry can be classified into two categories: linear models and computational fluid dynamic (CFD) models. Historically, linear models[4] have been popular within the wind industry because of their low use of computational resources. These models solve a linearized version of the equations that govern the motion of the fluids (Navier-Stokes equations). However, these linear models might not capture the influence of the terrain on the wind flow accurately, especially in complex terrain.[5] On the other hand, CFD models numerically solve the Navier-Stokes equations by making assumptions about the flow conditions. Different types of CFD models exist, which are mainly differentiated by the way they model the turbulence. The most popular CFD models in the wind energy industry utilizes the steady-state version of the Reynolds-Averaged Navier-Stokes (RANS) equations. RANS models have improved performance compared with linear models (Figure 1.1), while keeping the computational cost relatively low. More advanced CFD models, which are based on large-eddy simulations or unsteady RANS simulations, are commercially available for wind resource assessment. However, they are used to a lesser extent due to their high use of computational resources.[6] Therefore, the focus of this study is on steady-state RANS models.

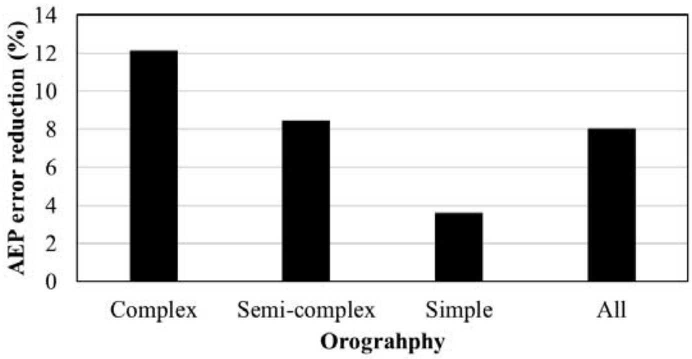

Figure 1.1. Average improvement of the estimated annual energy production (AEP) when using CFD versus linear models for 50 sites with different terrain complexity. Reproduced from Hristov et al. (2014).[7]

The wind flow solution obtained by a steady-state RANS model depends on the selected boundary conditions. These boundary conditions make explicit assumptions about the wind conditions, such as wind speed, wind direction, temperature and turbulence. In the wind energy industry, the boundary conditions are typically assumed to follow analytical formations based on the Monin-Obukhov similarity theory,[8] as well as to be invariant across the simulated domain. This way of prescribing boundary conditions, referred to in this study as standalone simulations, are sufficient for many wind energy projects. Nevertheless, they present important limitations in sites with complex weather systems, where real conditions can not only differ from this analytical formulation, but also present a significant spatial variation (Figure 1.2).

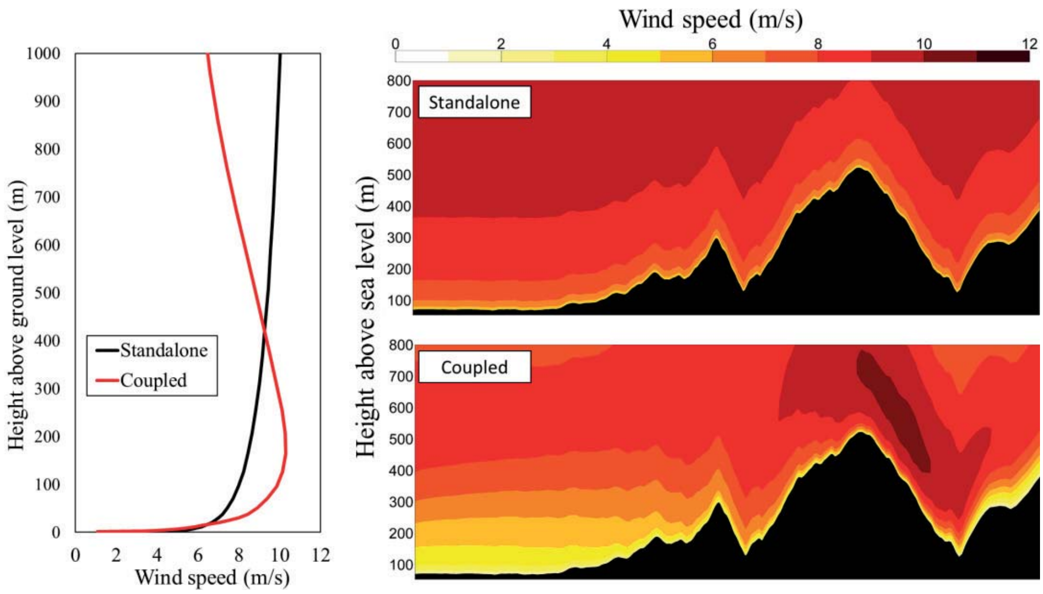

Figure 1.2. Comparison of the boundary conditions for standalone and coupled simulations. Left panel: comparison of the vertical profile of horizontal wind speed. Right panels: comparison of vertical planes of horizontal wind speed.

A necessary step towards improving steady-state microscale models is to have more realistic boundary conditions. The approach that is investigated in this thesis consists of computing the boundary conditions from models that can simulate the weather, the so-called mesoscale meteorological models (MMM). This approach is referred to in the literature as direct meso-microscale coupling.[6] Nested domains in the MMM are used to physically downscale the global circulation to the regional winds and then to the atmospheric boundary layer wind flow (Figure 1.3). It is expected that the wind flow solution of a direct meso-microscale coupling approach would benefit from both more realistic weather conditions by the MMM and from a proper inclusion of the local orography by the microscale model. Recently, publicly available mesoscale data have been published at the New European Wind Atlas database.[9] Other similar mesoscale simulation databases exist, like the Dutch Offshore Wind Atlas.[10] It is expected that this kind of databases will be increasingly common in the future, and in order to exploit them, the development of direct meso-scale coupling methodologies is required.

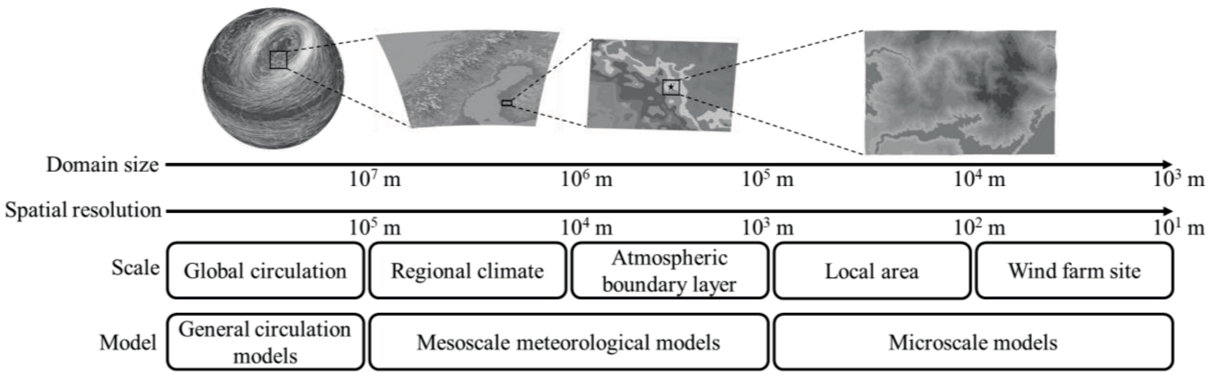

Figure 1.3. Spatial scale ranges of different wind flow modeling approaches. Adapted from Sanz et al. (2017).[6]

1.2 Brief review of meso-microscale coupling literature

As reported in Paper I, meso-microscale coupling models are widely studied within the wind modelling field. Most of the reviewed literature on meso-microscale coupling can be classified according to the modelling approach utilized at the microscale level:

i. Direct coupling using an unsteady microscale model like large-eddy simulations or unsteady RANS

ii. Direct coupling using a steady-state microscale model to simulate some timesteps

iii. Steady-state microscale model using analytical boundary conditions, which is then scaled by the mesoscale wind speed at a given grid point(s)

As previously mentioned, approach (i) is not feasible for most of the wind industry given the extensive use of computational resources; while approach (ii) is mostly used for urban studies (like pollution dispersion) in order to simulate a specific event. Approach (ii) cannot be applied for wind resource assessment since it would require simulating too many timesteps (for example, each hour of a year). Approach (iii) has applications in wind energy for site screening or for the elaboration of wind atlases. Nevertheless, this approach does not solve the problem of unrealistic boundary conditions as it also uses analytical boundary conditions to force the model, and the mesoscale results are only used to scale the model. In wind resource assessment, the scaling is typically conducted using onsite measurements, which are regarded as a better representation of real wind conditions.

There are two challenges when using direct meso-microscale coupling with steady-state models for wind resource assessment purposes. First, it is necessary to define how many and which mesoscale fields would be used to compute the boundary conditions. The idea is that the selected or computed fields are representative for the most predominant conditions at the site. Secondly, once having these representative mesoscale fields, a procedure to compute the boundary conditions is required. This is a problem that is commonly addressed by the studies that use approaches (i) and (ii), and much of their insights were used in this study. Nevertheless, in most of the studies the problem of finding representative mesoscale fields is typically not addressed. From the literature survey, the only work that deals with this problem is the study carried out by Duraisamy (2014).[11] In that study, the 3-D simulated mesoscale timeseries are classified using a *k*-means clustering approach, obtaining 64 fields that are then downscaled with a microscale model. The validation of the methodology in that study is rather limited as it is only applied at one site. Another shortcoming is that the applied clustering approach requires to define a priori the total number of clusters, which can lead to repeated or insufficient clusters. The study presented in this PhD is similar in the sense that classification approaches are applied to obtain representative mesoscale fields, which are then downscaled. However, this PhD thesis is focused as well on the automatization of the mesoscale classification and on a wider validation of the capabilities of the meso-microscale coupling models.

1.3 Objectives of the research

The aim of the research presented in this PhD thesis is to develop methodologies that enable the combined use of MMM simulations with steady-state RANS modelling for wind resource assessment applications. The main challenge of this meso-microscale coupling method is to cope with the different ways these models deal with time. MMM simulations are time dependent (also called transient), while steady-state RANS models are time independent. Thus, the challenge is to establish the number of coupled simulations needed to fairly represent the different conditions simulated by the MMM. This challenge is analogous to determining how many and which frames of a video are required to sufficiently convey the information contained in it.

It is expected that some information from the mesoscale simulation will be lost through the coupling procedure. On the one hand, the use of a steady-state model in the microscale will necessarily be unable to transfer transient phenomena, especially during unstable conditions. On the other hand, due to the simpler physics modeled by the RANS model used in this study, it is not possible to take into account the same physical processes as the mesoscale model.

Therefore, an additional objective of this study is to have a better understating of the limitations of the direct coupling methodologies developed. It is important to determine in a quantifiable manner which modelling approaches are more adequate for different types of terrain complexity, atmospheric stability conditions and local weather phenomena.

In summary, the specific objectives of this research are:

i. Develop meso-microscale coupling methodologies for steady-state microscale models that utilize a reasonable number of simulations (≤ 36)

ii. Quantify the gain in utilizing the developed meso-microscale coupling methodologies for different type of terrain and weather conditions

iii. Identify the limitations of the developed meso-microscale coupling methodologies and the possible solutions to further enable their use for wind resource assessment

In the research articles of this thesis, two meso-microscale coupling methodologies are developed. In Papers I and III, a directional average approach is utilized, while Papers II and IV utilizes an approach based on neural networks. Both methodologies comply with using a reasonable number of simulations. Furthermore, the approach based on neural networks achieve this in a fully automated manner. In the articles, the coupling methodologies are validated at different sites with a variety of terrain and wind conditions. The capability of the coupling methodology to downscale different mesoscale wind patterns is evaluated qualitatively and quantitatively.

1.4 Thesis outline

The remaining of the PhD thesis is structured as follows: In Chapter 2, all the materials and methodologies utilized through the research are presented. These consist of the datasets used for the modeling and validation of the studied sites, as well as their corresponding mesoscale simulations. In the same section, technical details are provided for the microscale model and for the meso-microscale coupling methodology. Finally, the error metric utilized in the validation study is described. To avoid repetition, detailed information presented in the research articles of this thesis are not repeated in this synopsis. This especially applies to the datasets of the validation sites, the coupling methodologies and the validation metric. In Chapter 3, the results and findings of the articles are summarized. The results are organized into three main topics: (i) capabilities of the classification techniques utilized, (ii) capabilities of the coupled simulations to downscale mesoscale patterns and (iii) validation study results.

This PhD thesis contains four research articles, and the relation between them is outlined in Figure 1.4. The research contained in these articles can be summarized as a development and validation of two meso-microscale coupling methodologies. The main difference between the methodologies is the procedure utilized to obtain the representative mesoscale fields. One of these methodologies correspond to a simple approach that consists of using the average values of the MMM variables to prescribe the boundary conditions to the microscale model, which is proposed and validated in Paper I. In parallel to this work, a more sophisticated classification methodology was proposed in Paper II. This classification methodology is based on a machine learning technique, called self-organizing maps (SOM), to obtain prevalent patterns in a dataset in a fully automated fashion. In Paper II, the focus was only on the classification methodology and on proving its capabilities in classifying relevant wind patterns, in particular, wind speed profiles. Paper III further develops the work of Paper I, by introducing some improvements and more importantly, making use of a larger sample of sites and observational points to validate the coupling methodology. Finally, Paper IV utilizes the same classification method developed in Paper II to obtain the predominant patterns of a mesoscale simulation. These patterns are downscaled and validated using an identical coupling methodology as in Paper III.

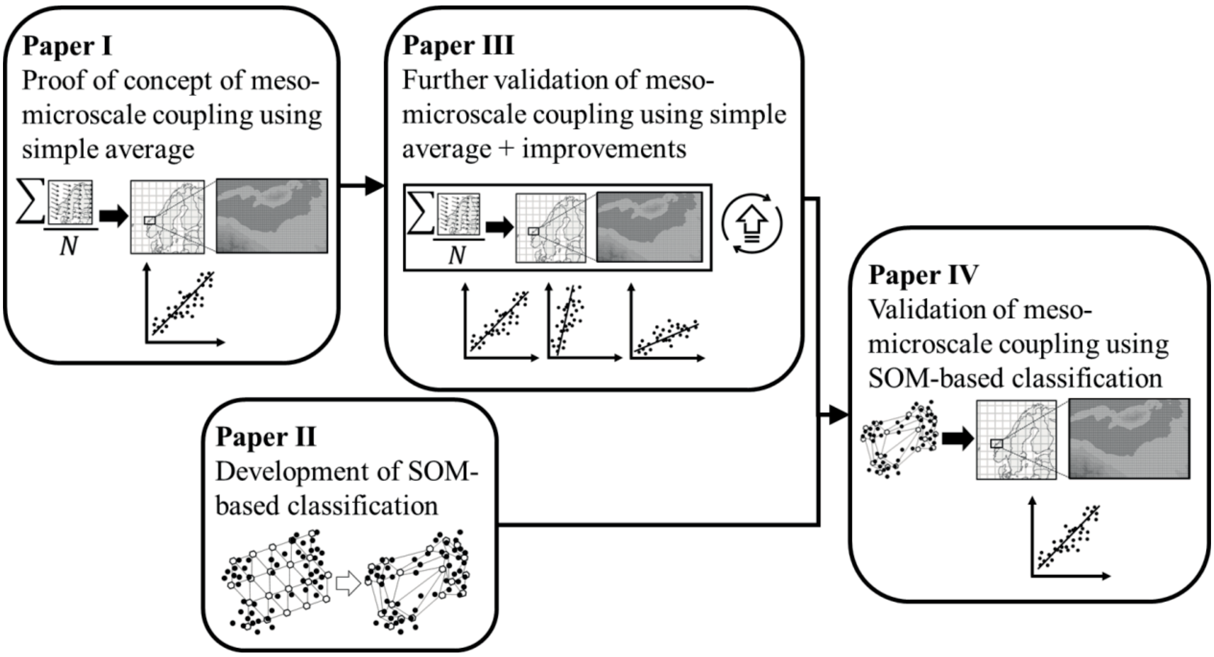

Figure 1.4. Relation of the research papers in this PhD thesis

Datasets and methodologies

The datasets and methodologies used to carry out this PhD study are presented in this chapter. In Figure 2.1, the relationship between these elements is outlined. The terrain datasets are utilized to build the digital terrain models of the microscale model of WindSim. This microscale model is coupled with the mesoscale simulations through a transferring procedure. The simulation results of this procedure are compared to the results of the standalone WindSim model, which are utilized as a benchmark. The results from both models are compared against onsite measurements using crosscheck prediction errors.

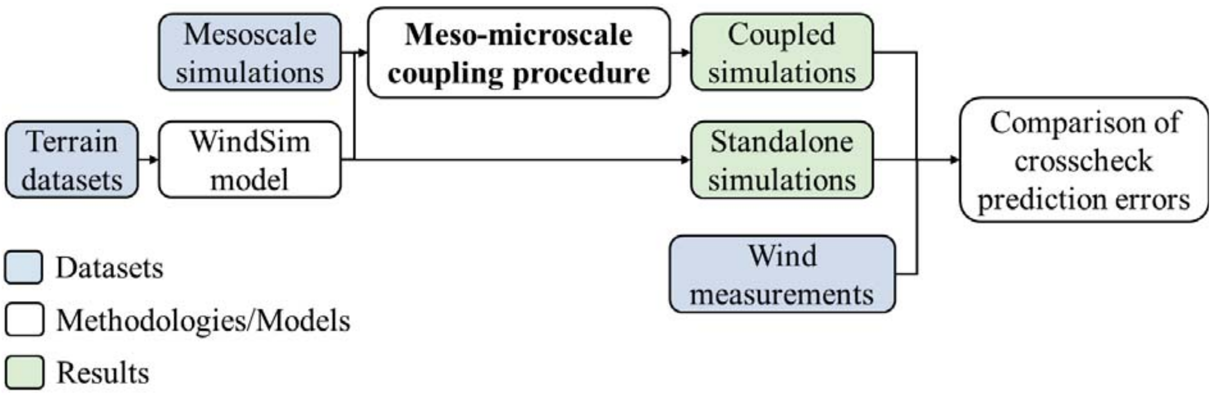

Figure 2.1. Relation of the models, methodologies and datasets used in this PhD thesis. The main contributions of the research are in the meso-microscale coupling procedure (indicated in bold).

The contributions of the research conducted in this thesis are mainly in the meso-microscale coupling procedures. Other minor contributions were introduced in the microscale modeling and in the crosscheck prediction error procedure of WindSim. Further technical details on the datasets, methodologies and models are provided in the following subsections.

2.1 Validation sites

Six sites, which are listed in Table 1, are used in this PhD study. All of them correspond to commercial wind energy generation projects in different states of development. Datasets from most of the projects were only provided for the purpose of this research, and therefore georeferenced data and absolute values of the measurements are not disclosed. The only site without restrictions regarding the datasets is Honkajoki. Non-public datasets for the Honkajoki and CA sites were provided by the Novia University of Applied Sciences in Finland and RWE Renewables Americas LLC in the US, respectively. The remaining datasets were provided by Mainstream Renewable Power in Chile.

Table 1. Validation sites used in the research articles of this PhD thesis.

Name	Location	Meteorological conditions	Paper
Honkajoki	Finland	Very stable conditions	I
CM	Southern Cone	Near-neutral to stable conditions	III
CA	North America	Very stable conditions	III
CL	Southern Cone	Strong day-night cycle	III
CK	Southern Cone	Strong day-night cycle	III and IV
PS	Southern Cone	Near-neutral to stable conditions	III

None of the projects presented in Table 1 were utilized in Paper II. Instead, the locations of the FINO-1 and Cabauw meteorological towers were used. Due to the nature and scope of Paper II, no measurements were required, and these locations were only used because they are well-known experiments in the wind energy community. For each of the sites listed in Table 1, three kinds of datasets are used to carry out the study:

1) Wind measurements
2) Terrain
3) Mesoscale simulations

An overview of the datasets is presented in Figures 2.2-2.7. In the following subsections details of the datasets are provided.

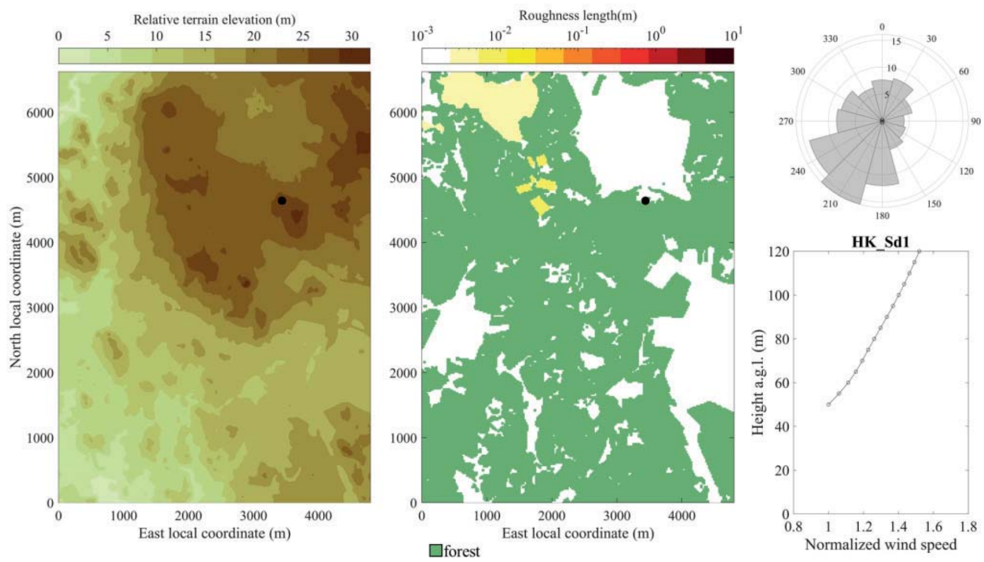

Figure 2.2. Terrain and wind characteristics at the Honkajoki site. The locations of the measurement are indicated by black circles in the maps. Polar and radial axis of the wind rose correspond to the wind direction (°) and frequency (%), respectively. The instrument used to compute the wind characteristics is indicated above of the bottom-right panel.

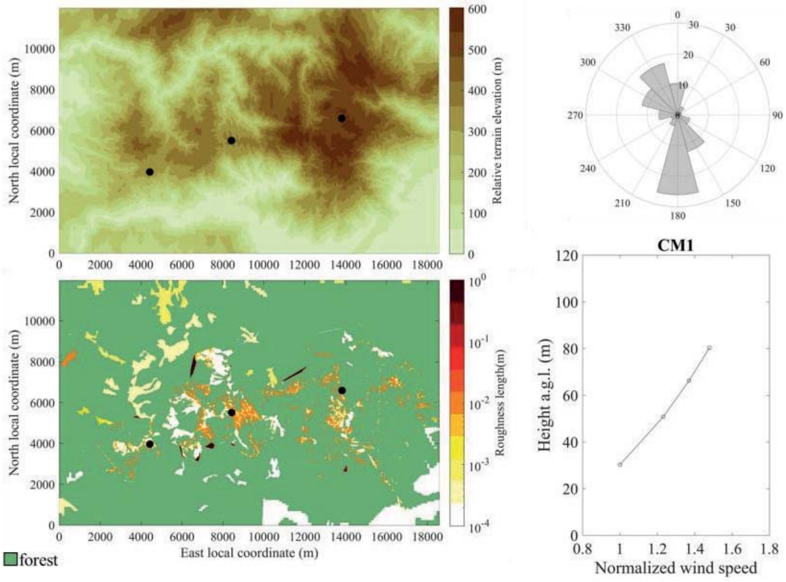

Figure 2.3. Same as Figure 2.2 but for the CM site.

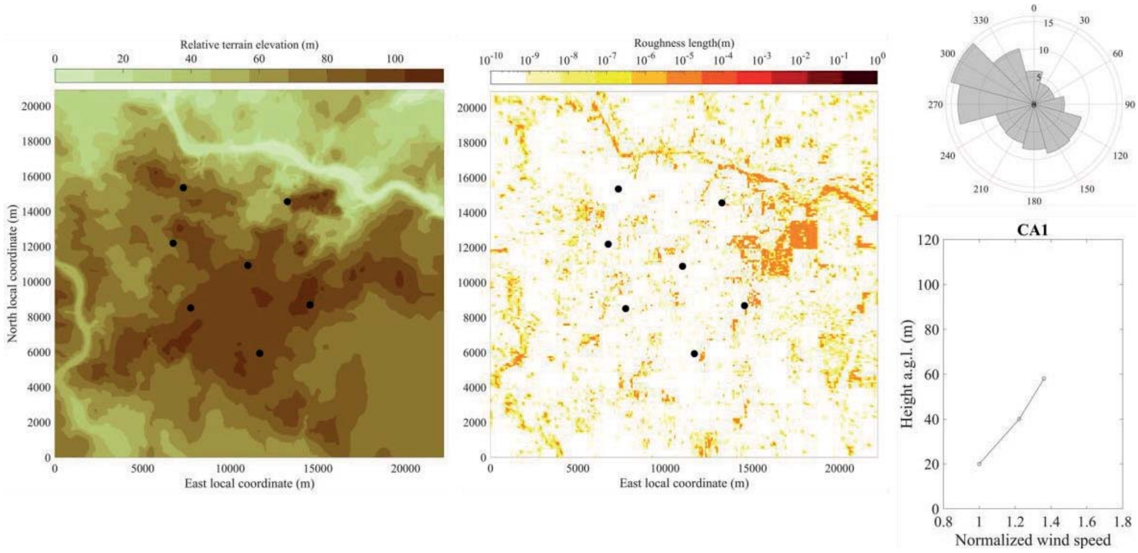

Figure 2.4. Same as Figure 2.2 but for the CA site.

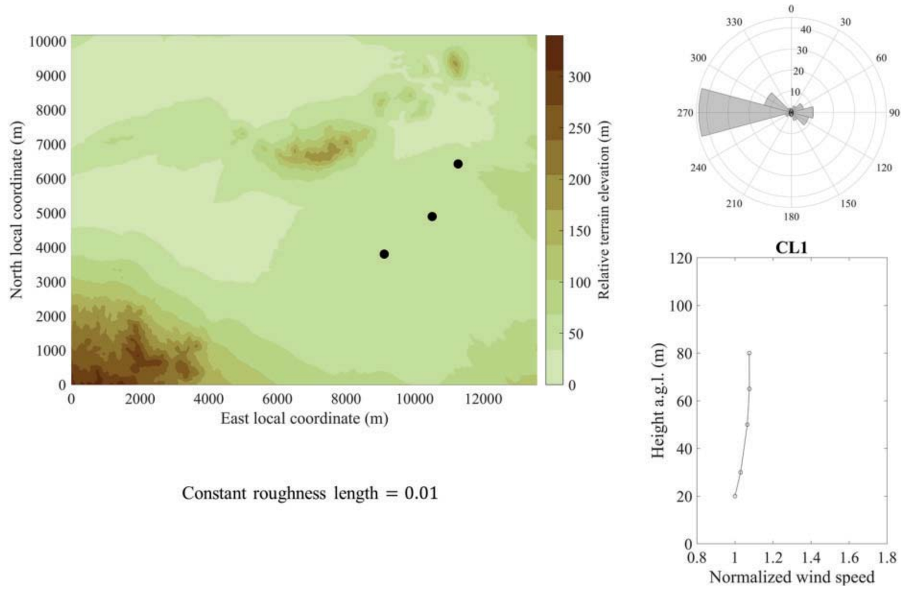

Figure 2.5. Same as Figure 2.2 but for the CL site.

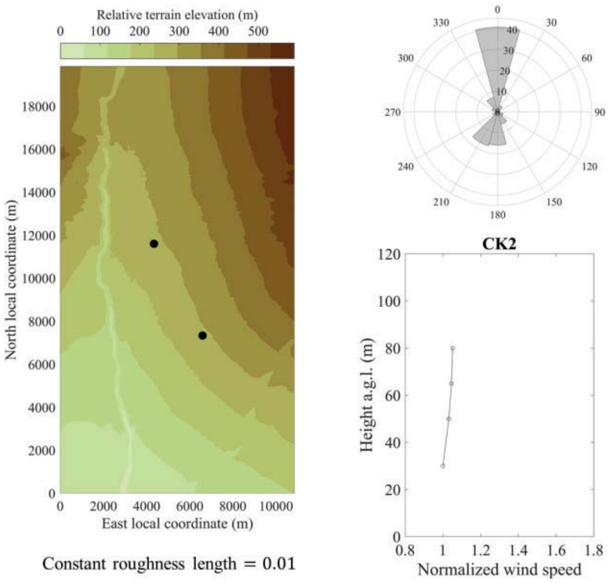

Figure 2.6. Same as Figure 2.2 but for the CK site.

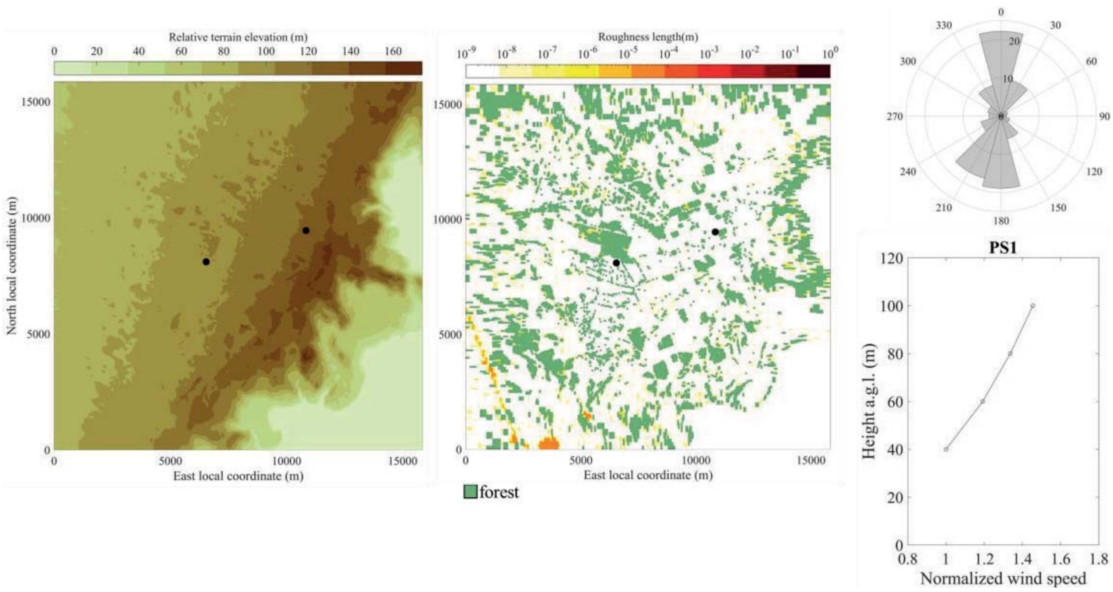

Figure 2.7. Same as Figure 2.2 but for the PS site.

2.1.1 Wind measurements

Onsite measurements of the wind conditions at the sites were obtained through different instruments. The type of instruments utilized for these measurements are some of the ones typically used for wind resource assessment: cup anemometers, wind vanes and light detection and ranging (LiDAR) systems (Figure 2.8). The measured variables that are used in the validation studies of this thesis are the wind speed and wind direction, which are averaged every 10 minutes. Other measured variables that were not directly used in the study include turbulence intensity (or standard deviation of the wind speed), vertical wind speed, temperature, humidity and pressure. Most of these variables are used for suitability studies and energy yield calculations, which are beyond the scope of this work.

Figure 2.8. Instruments utilized at the CL site. Left and center panels: Anemometer and wind vane, respectively, mounted in a meteorological mast. Right panel: Deployed LiDAR. Courtesy of Mainstream Renewable Power.

Cup anemometers and wind vanes were calibrated using the parameters provided by external laboratories. The data collected from cup anemometers and wind vanes are cleaned for invalid or unrealistic values, as well as for icing events, utilizing the Windographer software (Figure 2.9). Cup anemometers and wind vanes are mounted into meteorological masts. Usually two anemometers are mounted per vertical level in order to prevent tower distortion (Figure 2.10). The data from both anemometers are combined into one timeseries, which considers the mast wake for a given range of wind directions.

The data collected by the LiDARs is already filtered from low quality measurements by the software included in the instrument. The data from some LiDAR brands had to be cleaned or corrected due to improper wind direction measurement. Further details on the type and number of instruments per site can be found in Papers I, III and IV.

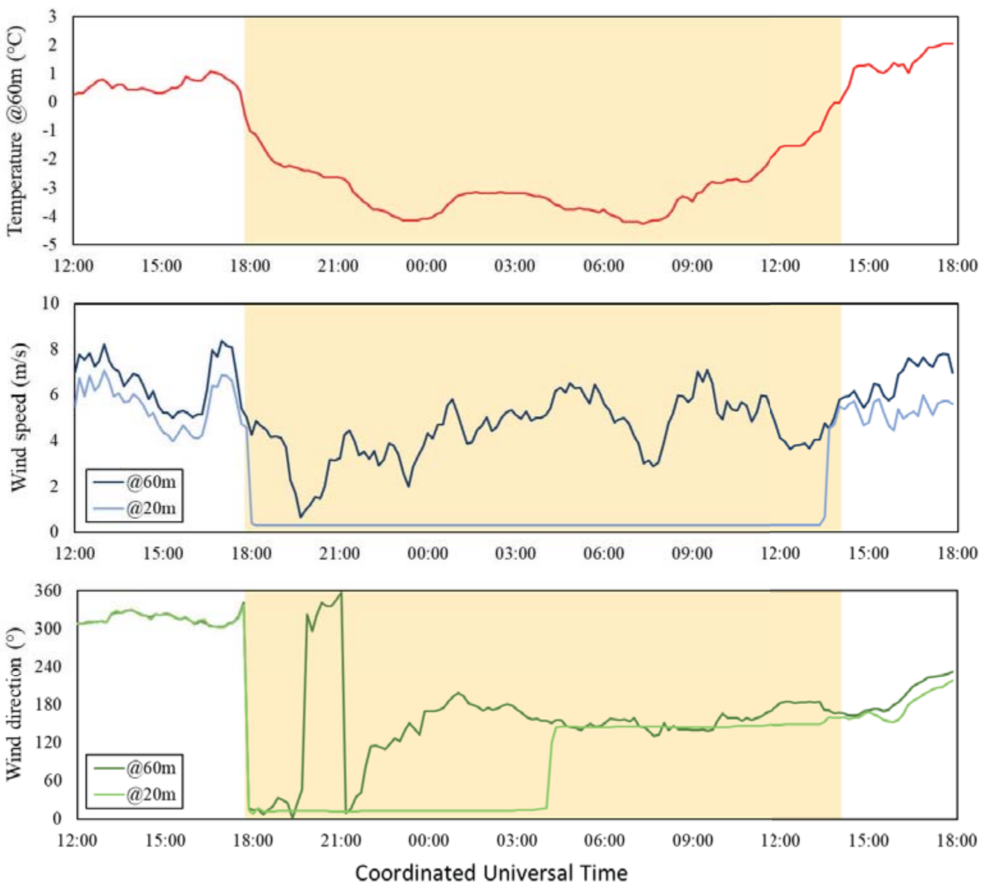

Figure 2.9. Example of an icing event (indicated in yellow). The cup anemometer and the wind vane @20m are affected by icing. Instruments @60m may also be partially affected by icing. Temperature and/or humidity measurements help to identify icing events.

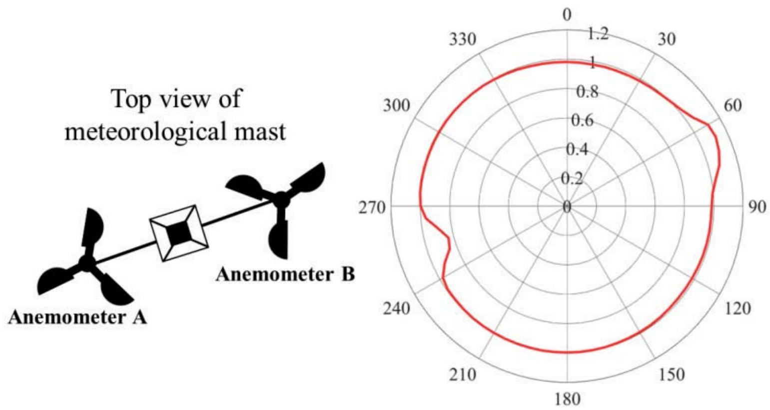

Figure 2.10. Example of tower distortion of measurements. The red line indicates the average ratio between the wind speed measured at anemometers B and A (radial axis) for a given wind direction (polar axis).

The measurement campaign of each site complies with the standards of the International Electrotechnical Commission, Measnet and/or other local standards. Out of the studied sites, Honkajoki is the only one that has measurements in just one location. For this reason, validations at this site were only possible in the vertical direction. The sites Honkajoki, CM and CA present a high wind shear (Figures 2.2, 2.3 and 2.4), while the sites CL and CK present low wind shear (Figures 2.5 and 2.6). Both conditions are likely to be related to the predominant atmospheric stability conditions at the sites. Among them, Honkajoki and CA are the sites where the wind is the most evenly distributed between the different wind directions (Figures 2.2 and 2.4). The opposite is true for the CL and CK sites, where the wind mostly comes from one wind direction (Figures 2.5 and 2.6).

2.1.2 Digital terrain model

The most important factors that influence the behavior of the local wind flow are related to the terrain conditions. These conditions are represented in the digital terrain model of the site, which consists of a 2-D grid of point values of terrain elevation and roughness length. In forested sites additional information is required, which consist of the location of the forest, canopy height, forest sparsity and tree species. In the WindSim model, this information is used to set certain grid cells of the model as forest by defining them as a semi-permeable obstacle. More details on the forest modelling are provided in Section 2.2.

For the sites of this PhD thesis, the terrain elevation was obtained from the databases of the Shuttle Radar Topography Mission,[12] the Canadian Digital Elevation Data,[13] the Finish National Land Survey[14] and from LiDAR campaigns conducted by the project owner or commercial providers, like WorldDEM. Roughness length maps are constructed from land cover maps obtained from open databases like the GlobeLand30,[15] the US National Land Cover Database 2001[16] and/or commercial sources. These land cover maps are translated into roughness maps following conversion tables, usually based on the work of Davenport (1960).[17] In the case of the CL and CK sites, a constant roughness value for the entire domain is used instead, as they present a very homogeneous terrain type and more detailed information of the terrain is not available in the aforementioned databases. Further characteristics of the digital terrain models can be found in Papers I, III and IV.

There is a wide variety of terrain complexity among the modeled sites. Honkajoki and CA have a relatively flat terrain (Figures 2.2 and 2.4). CL and PS also present a relatively flat terrain, but with some hilly areas and other terrain features (Figures 2.5 and 2.7). The terrain of the CK site is relatively even with an overall inclination towards the north (Figure 2.6). By far, the most complex site is CM (Figure 2.3).

2.1.3 Mesoscale simulations

About one-year worth of mesoscale simulations are available for each of the modelled locations. These simulations were produced using the Weather Research Forecasting (WRF) model.[18] Depending on the site, the runs were conducted by the High Performance Computing Center North (HPC2N),[19] Vortex SL[20] or one of the co-authors of Paper II (Table 2). Further technical details about the settings of the WRF simulations are provided in Papers I, II and III. The postprocessing of the results was conducted using a time resolution of 1 hr for the outputs. The simulated periods were selected in order to cover the longest concurrent period measured at all observational points at each site.

Table 2. Source of the WRF simulations utilized in the research articles of this thesis.

Site	WRF version	Conducted by
Honkajoki	3.7.1	HPC2N
FINO-1	3.6.1	Co-author in paper
Cabauw	3.6.1	Co-author in paper
CM	3.7.1	Vortex SL
CA	3.7.1	Vortex SL
CL	3.7.1	Vortex SL
CK	3.7.1	Vortex SL
PS	3.7.1	Vortex SL

2.2 WindSim

In this study, the steady-state RANS model that is part of the commercial software WindSim is utilized as a microscale model. The model predicts the spatial perturbations of the wind speed for a given set of boundary conditions. For wind resource assessment applications, it is assumed that the solution of the model is Reynolds number independent, i.e. the spatial wind perturbations are independent of the wind speed. For example, if the model predicts variation of X% in the wind speed between point A and point B, this percentual change is independent of the wind speed at point A. However, wind speed perturbations are still dependent on the direction of the wind, and therefore several simulations with different wind directions are typically conducted to assess a site.

The governing equations of the WindSim's CFD model correspond to the RANS equations,[21] assuming steady-state (derivatives in time =0) and incompressibility (constant density). All equations in this subsection are given in Einstein notation. Sub-indexes $i, j = 1, 2, 3$ correspond to north, east and vertical components, respectively. Mass conservation is expressed as:

$$\frac{\partial U_i}{\partial x_i} = 0 \tag{1}$$

where U_i and x_i correspond to the i-component of the wind speed vector and of the cartesian coordinate, respectively. The conservation of momentum in the horizontal direction is expressed as:

$$U_j \frac{\partial U_i}{\partial x_j} = -\frac{1}{\rho}\frac{\partial P}{\partial x_i} + \frac{\partial}{\partial x_j}\left(\nu\left(\frac{\partial U_i}{\partial x_j} + \frac{\partial U_j}{\partial x_i}\right) - \left(\overline{u_\iota u_J}\right)\right) \qquad i = 1,2 \tag{2}$$

where P is the pressure, ρ is the air density and ν is the air viscosity. The conservation of momentum in the vertical direction has an additional forcing term when thermal effects (atmospheric stability) are present:

$$U_j \frac{\partial U_3}{\partial x_j} = \frac{\theta_0 - \theta}{\theta_0} g - \frac{1}{\rho}\frac{\partial P}{\partial x_3} + \frac{\partial}{\partial x_j}\left(\nu\left(\frac{\partial U_3}{\partial x_j} + \frac{\partial U_j}{\partial x_3}\right) - \left(\overline{u_3 u_J}\right)\right) \tag{3}$$

where g is the gravitational acceleration, θ is the potential temperature and θ_0 its reference value. For neutral simulations $\theta = \theta_0$ and therefore the extra forcing term =0. The potential temperature is influenced by advection, thermal diffusion and turbulent heat transfer, expressed as:

$$U_i \frac{\partial \theta}{\partial x_i} = \frac{\partial}{\partial x_i}\left(\alpha\left(\frac{\partial \theta}{\partial x_i}\right) - \left(\overline{u_\iota \theta'}\right)\right) \tag{4}$$

where α is the kinematic molecular diffusivity for heat in air. The turbulent terms in Equations (2), (3) and (4) are parametrized as:

$$\left(\overline{u_\iota u_J}\right) = -\nu_T\left(\frac{\partial U_i}{\partial x_j} + \frac{\partial U_j}{\partial x_i}\right) + \frac{2}{3}\delta_{i,j} \tag{5}$$

$$\left(\overline{u_\iota \theta'}\right) = \frac{-\nu_T}{\sigma_\theta}\left(\frac{\partial \theta}{\partial x_i}\right) \tag{6}$$

where $\delta_{i,j}$ is the Kronecker delta and $\sigma_\theta(=1)$ is the turbulent Prandtl number for heat transfer. The turbulence viscosity ν_T is obtained from the standard $k-\varepsilon$ turbulence model as formulated by Lauder and Spalding (1974):[22]

$$\nu_T = c_\mu \frac{k^2}{\varepsilon} \tag{7}$$

$$\frac{\partial(U_i k)}{\partial x_i} = \frac{\partial}{\partial x_i}\left(\frac{\nu_T}{\sigma_k}\frac{\partial k}{\partial x_i}\right) + P_k + P_b - \varepsilon \tag{8}$$

$$\frac{\partial(U_i \varepsilon)}{\partial x_i} = \frac{\partial}{\partial x_i}\left(\frac{\nu_T}{\sigma_\varepsilon}\frac{\partial \varepsilon}{\partial x_i}\right) + c_{\varepsilon 1}\frac{\varepsilon}{k}(P_k + c_{\varepsilon 3}P_b) - c_{\varepsilon 2}\frac{\varepsilon^2}{k} \tag{9}$$

$$P_k = \nu_T \left(\frac{\partial U_i}{\partial x_j} + \frac{\partial U_j}{\partial x_i}\right)\frac{\partial U_i}{\partial x_j} \tag{10}$$

$$P_b = -\frac{\nu_T}{\sigma_\theta} g \frac{1}{\theta}\frac{\partial \theta}{\partial x_3} \tag{11}$$

Here k corresponds to the turbulent kinetic energy (TKE) and ε to its dissipation rate (EDR). The values of the model constants c_μ, σ_k, σ_ε, $c_{\varepsilon 1}$, $c_{\varepsilon 2}$ and $c_{\varepsilon 3}$ are presented in Table 3. The term P_b is used in Equation (8) when thermal effects are present, otherwise $P_b = 0$.

Table 3. Values of the model constants of the standard $k-\varepsilon$ turbulence model used by Lauder and Spalding (1974).[23]

c_μ	σ_k	σ_ε	$c_{\varepsilon 1}$	$c_{\varepsilon 2}$	$c_{\varepsilon 3}$
0.09	1.0	1.3	1.44	1.92	1.0

Since the potential temperature gradients in coupled simulations can be much more stably stratified than the analytical formulations, some limits were introduced to the values of P_b. In order to prevent too low turbulence in very stable conditions, P_b is limited in Equation (8) by $P_b = \max(-Rf_c P_k, P_b)$, where $Rf_c = 1 - c_{\varepsilon 1}/c_{\varepsilon 3} = 0.25$.[24] On the other hand, P_b is limited in Equation (9) by $P_b = \max(0, P_b)$.[25] These limits were used introduced Paper III and also used in Paper IV. Further justification of this addition is provided in Paper III.

In WindSim, forest is modelled by defining the grid-cells where it is located as a porous media. Therefore, source/sink terms S_j, S_k and S_ε are added at the right side of the governing equations of momentum (Equation (2) and (3)), TKE (Equation (8)) and EDR (Equation (9)), respectively. These terms are parametrized as:[26]

$$S_j = -\rho C_d \sqrt{U_i U_i} U_j \tag{12}$$

$$S_k = C_d\left(\beta_p \sqrt{U_i U_i}^3 - \beta_d U_i k\right) \tag{13}$$

$$S_\varepsilon = C_d\left(c_{\varepsilon 4}\beta_p \frac{\varepsilon}{k} U_i^3 - c_{\varepsilon 5}\beta_d U_i \varepsilon\right) \tag{14}$$

where C_d is the drag coefficient of the forest and β_p, β_d, $c_{\varepsilon 4}$, and $c_{\varepsilon 5}$ are model constants, whose values are shown in Table 4. C_d values are chosen for each grid-cell defined as forest, depending on tree sparsity, tree species and the geographical location of the forest.

Table 4. Values of the forest constants according to the formulations of Sanz (2003)[27] using the model constants in Table 3.

β_p	β_d	$c_{\varepsilon 4}$	$c_{\varepsilon 5}$
1	6.51	1.24	1.24

2.3 Meso-microscale coupling procedure

The meso-microscale coupling procedure consists of two steps. First, a set of mesoscale fields that are representative of the predominant wind conditions at the site are obtained. Secondly, these representative mesoscale fields are transferred into the microscale model as boundary conditions. Paper II is focused only on the first step, while the other papers deal with both. Details about the procedures utilized at each step are provided in the following sections.

2.3.1 Computation of representative mesoscale fields

In this PhD thesis, two methodologies were proposed to obtain representative mesoscale fields. One consists of averaging the wind conditions per directional sector, while the other obtains these conditions in an automated fashion utilizing neural networks. The first approach is regarded as a simple method that resembles the normal modeling approach used in the wind industry (one simulation per directional sector). The second method requires a further understanding of the abstraction done by the neural map. Nevertheless, it provides a powerful tool to easily explore the wind conditions that occur in a site in a comprehensive manner.

A common procedure for both methodologies is to filter timesteps that have an average wind speed below 3 m/s, for all grid points between 50 and 150 m a.g.l. and that lie within the microscale domain. This way, all mesoscale timesteps that are not of interest for wind energy generation are filtered out. The variables of interest of the obtained mesoscale fields are $U_i (i = 1,2,3)$, θ and the planetary boundary layer height.

2.3.1.1 Directional average

The first methodology proposed in this study consists in averaging all timesteps of the mesoscale simulation timeseries according to their wind direction. This procedure generates one representative wind condition per desired wind direction. The approach implicitly assumes that the wind conditions for a given wind direction are relatively similar in time. This assumption holds true in many wind energy projects, especially at sites where the wind rose is well spread across wind directions or if the site is strongly influenced by sea-land or mountain-valley winds.[28,29] In any case, this assumption is also made when running a standalone microscale model. Therefore, the use of this methodology does not present additional assumptions with respect to the normal application of the microscale model in wind resource assessment. It is expected that by downscaling the obtained mesoscale fields, the wind flow solution will be better for wind directions strongly influenced by mesoscale circulations (Figure 2.11).

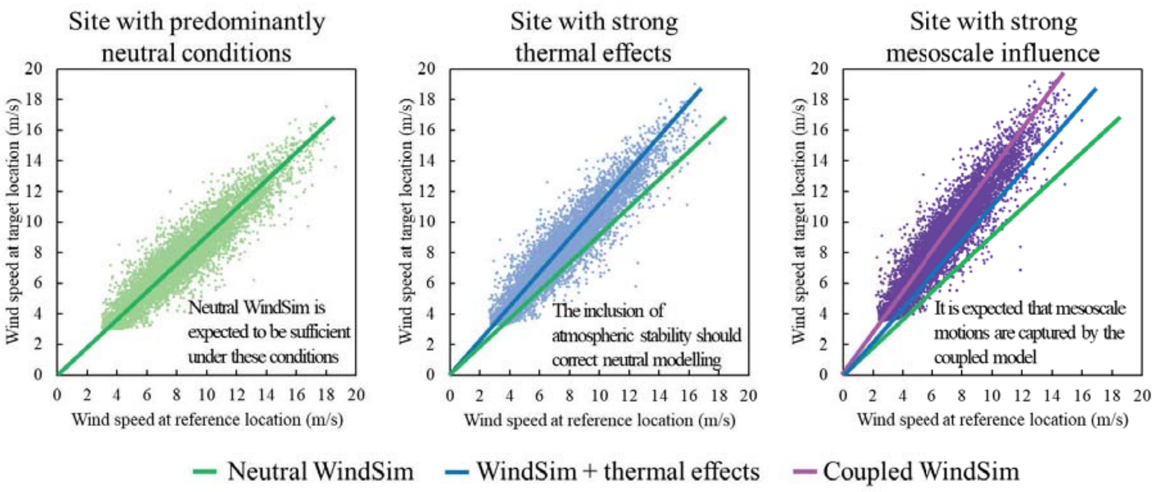

Figure 2.11. Expected application of different microscale modelling approaches. The dots correspond to onsite measurements and the lines to the prediction of the model.

Further technical details on the averaging procedure are provided in Papers I and III. The differences between the procedures used in those papers are presented here. In Paper I, the mesoscale fields of θ are directly averaged, while in Paper III the values of θ_0 and $\Delta\theta = \theta - \theta_0$ are separately averaged instead. Then, the average field of θ is calculated as $\bar{\theta} = \overline{\Delta\theta} + \overline{\theta_0}$. This second approach better captures the average atmospheric stability condition (contained in $\Delta\theta$) as it is not distorted by its absolute value. On the other hand, the mesoscale fields in Paper I are classified by their atmospheric stability in addition the wind direction. Due to the small gain in model performance compared to the extra use of computational resources, as well as difficulties in classifying onsite measurements by atmospheric stability, the method was not pursued in Paper III. A final difference is that in Paper III an additional coupling approach was introduced, which consists in filtering the θ mesoscale fields. In the same paper this approach is compared with coupled models without temperature filtering and without using the temperature fields at all.

2.3.1.2 Two-level SOM clustering

The second methodology proposed in this PhD to obtain representative mesoscale fields is based on a self-organizing map (SOM).[30] A SOM is a grid of interconnected nodes that are positioned in the space of the input data (Figure 2.12). The positions of the SOM nodes are iteratively modified in such a manner that the nodes are transferred closer to locations with a high density of input data points and further away from data-sparse areas (Figure 2.12c). This procedure is called training and it is repeated up to a prescribed number of iterations. Once the SOM is trained, it is possible to visualize the clustering structures of the data by plotting the distance between each node and its neighbors (Figure 2.12d).

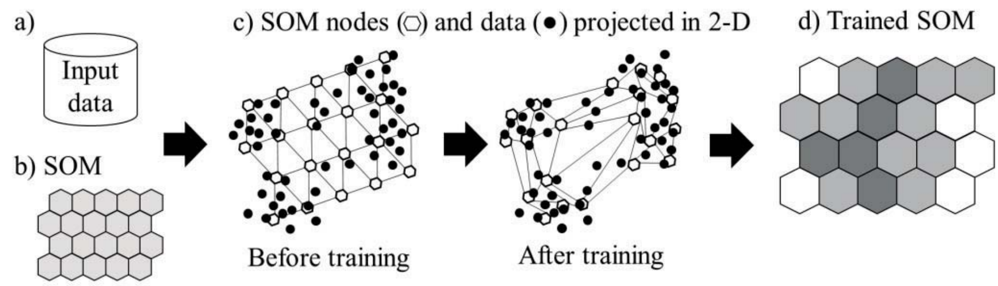

Figure 2.12. Example of the SOM training procedure with a dataset with 20 nodes and three clusters. Darker (lighter) shading in the SOM before (b) and after (d) training represents longer (shorter) distances between the node and its neighbors. Reproduced from Paper II.

As commented in the literature survey conducted in Paper II, most of the studies in meteorology that use SOM, directly use the nodes as a clustering solution. Nevertheless, such an approach presents certain problems. First of all, there is a practical constraint regarding the possible number of obtainable clusters, as the SOM can only be composed of a non-prime number of nodes. Additionally, neighboring nodes portray similar characteristics and therefore redundant patterns would be obtained. A more conceptual problem of this approach, as pointed out by Wu & Chow (2004),[31] is that the purpose of a SOM is to extract and visually display the structure of the input data, while clustering is to partition the input data into groups. The previously mentioned studies that directly use the nodes to cluster seem to mix these two objectives.

An important feature of SOMs is that the map preserves topological ordering. In other words, the nodes that are located close to each other share certain traits. For the context of this study, this implies that neighboring nodes share similar wind speed, wind shear, temperature shear and/or other characteristics (see for example Figure 2.13). This feature facilitates the characterization and understanding of the different conditions that occur in a site. By plotting different variables, it is possible to find relations (typically non-linear) among the different variables. For example, in Figure 2.13 it is possible to visually relate the speed and direction of the wind with the atmospheric stability conditions at the site.

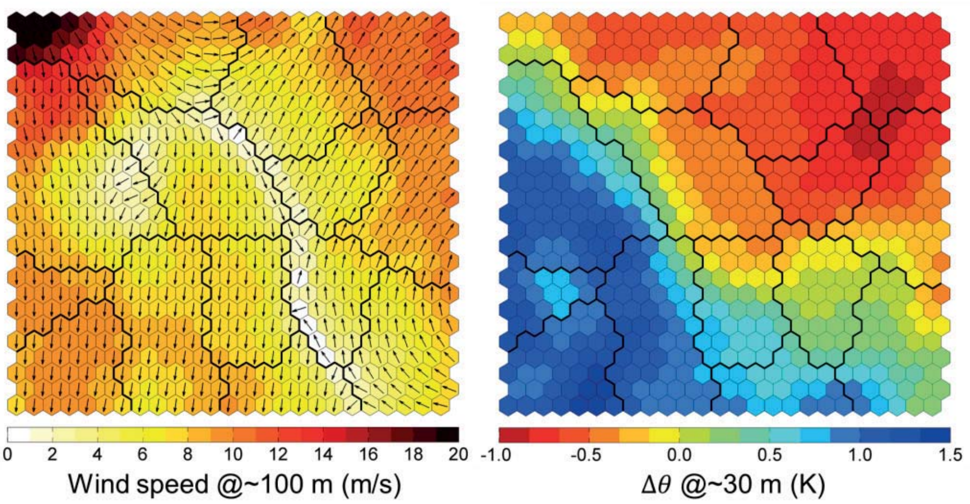

Figure 2.13. Representative wind speed (left) and $\Delta\theta$ (right) values of the nodes of a SOM of dimensions 25 × 25 used to classify WRF-simulated 3-D mesoscale fields at CK. The wind direction in the left panel is indicated by black arrows. The SOM partition is indicated by black lines. Adapted from Paper IV.

In order to use the SOM for clustering purposes, a two-level SOM clustering (SOM2L)[32] approach is utilized. The SOM2L consists of partitioning (i.e. clustering) the nodes of the SOM (as illustrated in Figure 2.13). Several clustering techniques can be used for this stage, like *k*-means or hierarchical clustering. The disadvantage of using these techniques is that the total number of clusters has to be prescribed a priori. Therefore, in this study it has been opted instead for a methodology that exploits the topological ordering of the SOM. Specifically, the cluster centers are defined as the local minima of the distance between each node and its neighbors (Figure 2.14).[33] The remainder of the SOM nodes are then assigned to a cluster following Ward's criterion.[34]

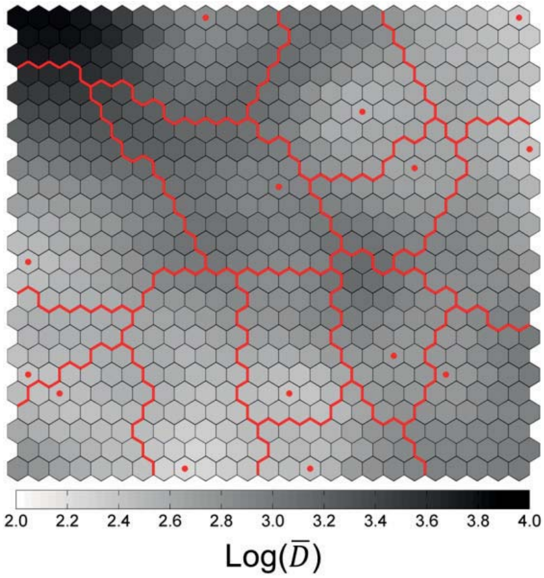

Figure 2.14. Partition of the SOM based on the local minima of $\bar{D}$. The local minima are indicated by the red dots and the partitions by the red lines. $\bar{D}$ corresponds to the average distance between a node and its neighbors. Reproduced from Paper IV.

As a result, the application of the SOM2L methodology to the mesoscale simulations provides a set of mesoscale patterns. If the input data correspond to 3-D mesoscale fields (as in Paper IV), these patterns represent a variety of the predominant wind conditions at the site. In contrast to the method that uses the directional averages explained in section 2.3.1.1, the patterns obtained with the SOM2L can yield several wind conditions for the same wind direction (Figure 2.15). Moreover, very infrequent wind directions will not be found in the extracted patterns. Further technical details of the parameters used in the SOM2L are provided in Paper II and IV. Detailed justification of the selection of these parameters are provided in Paper II and the references therein. As argued by Vesanto and Sulkava (2002),[33] the distance map "may have some local minima which are a product of random variations in the data". In order to prevent this, in Paper IV a smoothening function is applied to the distance map before computing the local minima.

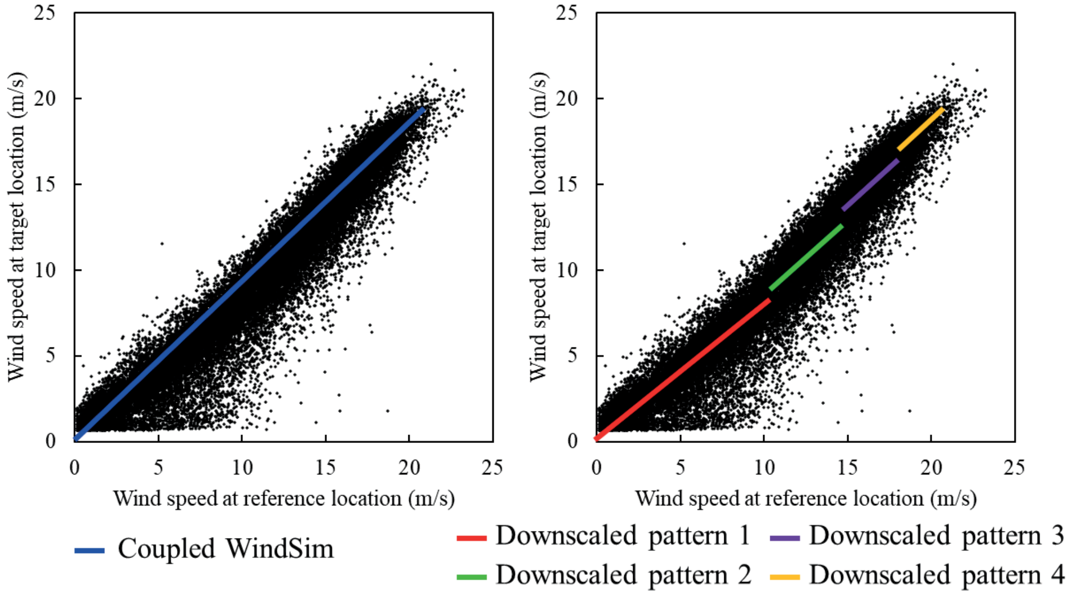

Figure 2.15. Conceptual comparison between the directional average coupling of section 2.3.1.1 (left) and the SOML2 coupling (right) for one directional sector. The dots correspond to onsite measurements and the lines to the prediction of the model.

2.3.2 Transferring of mesoscale fields to the microscale model

Once representative mesoscale fields are obtained, they are transferred into the microscale model as boundary conditions. There are six variables that are prescribed as boundary conditions: U_1, U_2, U_3, θ, k and ε. The values of U_1, U_2, U_3 and θ are computed by interpolating the mesoscale values onto the microscale grid. Vertical interpolations are first conducted utilizing the cubic spline method. Then, horizontal bilinear interpolations are conducted. If the interpolations are conducted in the inverse order (horizontal first, vertical second) the interpolated values might have some discontinuities, especially close to the ground.

The lowest vertical level of the WRF simulations results are typically located at approximately 10 m above the ground. It is very common that a few grid points of the microscale model are located bellow this height. Therefore, the WRF values of U_1, U_2 and θ are extrapolated using Monin-Obukhov similarity theory equations[8] with the two lowest vertical levels of the WRF domain, located at ~10 m and ~30 m. To compute the necessary parameters like the Monin-Obukhov length or the friction velocity, the gradient method[35] is utilized. In few occasions, this method is not applicable because of very low winds speeds and/or very high temperature gradients.[36] In these cases, the values are obtained from the average of the surrounding grid points. The values of vertical wind speed are simple prescribed as $U_3 = 0$.

The values of k and ε are computed using the analytical formulas derived by Han et al. (2000).[37] These formulas are also based in the Monin-Obukhov similarity theory. Most of the parameters required to apply these formulas are the same as the ones utilized in the extrapolations. In addition, the planetary boundary layer (PBL) height values transferred from the mesoscale are utilized. These values are obtained by horizontally interpolating the PBL height from the mesoscale simulations.

Further technical details of the interpolation and extrapolation procedures, as well as on the computation of k and ε are provided in Paper I. In Papers III and IV, the methods to compute the values are very similar. The only difference is that in Paper I the θ values are interpolated with respect to the height above ground level (a.g.l.), while in Papers III and IV they are interpolated with respect to the height above sea level (a.s.l.). As shown in Figure 2.16 the approach used to interpolate θ has an important impact in its vertical structure. It is important to preserve the PBL height transferred from the mesoscale (implicitly in the contained in the θ field) since the top of the PBL blocks the vertical motion of the flow. The site used in Paper I (Honkajoki) is very flat and therefore the θ field is barely distorted. In Paper III, most of the sites have a more complex terrain than Honkajoki, which made necessary to introduce this improvement in the interpolation procedure.

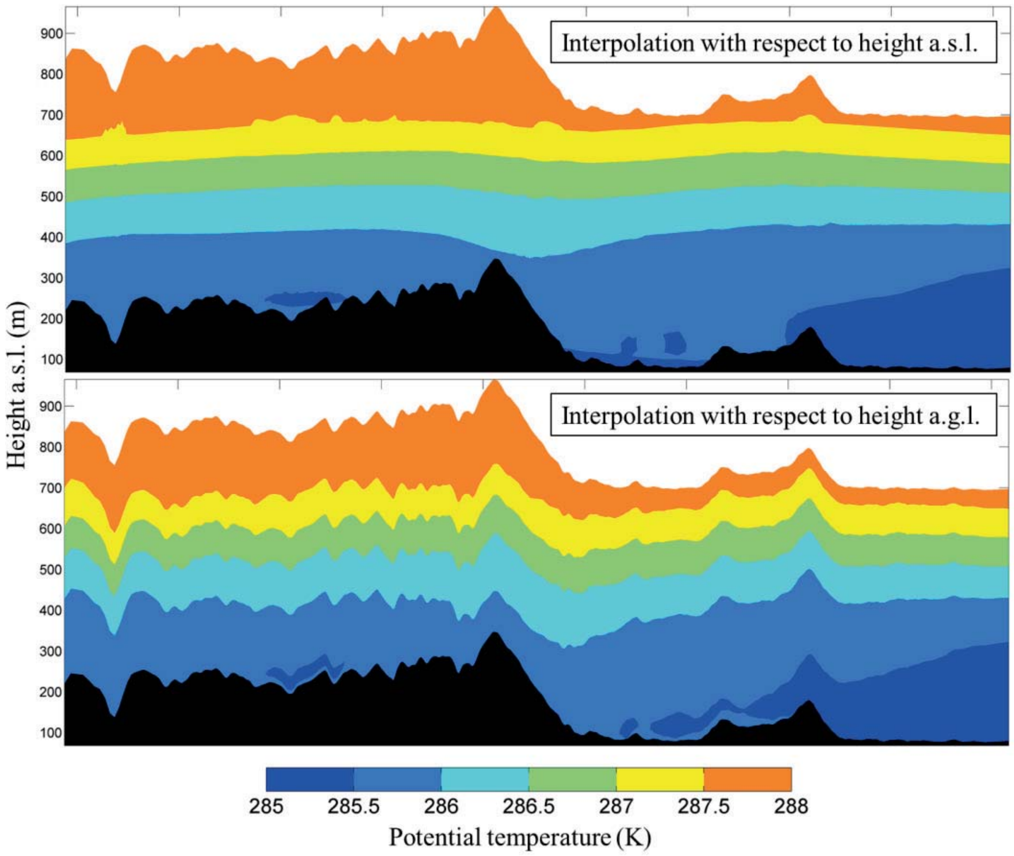

Figure 2.16. Comparison of vertical planes of potential temperature for different interpolation procedures.

2.4 Validation metric

As mentioned in Section 1.1, the purpose of the wind flow simulations in wind resource assessment is to extrapolate the wind measurements. These extrapolations consist in obtaining the wind speed at a target location T (typically a wind turbine) by multiplying the measured wind speed at a reference point R by a factor (Figure 2.17b). This factor is called the speed-up ratio SU, and it is calculated as:

$$SU(R,T) = \frac{u_T}{u_R} \tag{15}$$

where u_R and u_T are the modeled wind speeds at points R and T (Figure 2.17a). Therefore, the performance of a model is quantitatively evaluated by comparing the modeled SU with the measured one, between selected pairs of measurements. Specifically, the mean values of SU and wind speeds are utilized to calculate the so-called crosscheck prediction XPE as:

$$XPE(R,T) = \frac{\overline{SU(R,T)} \times \overline{u_R} - \overline{u_T}}{\overline{u_T}} \tag{16}$$

It is possible to calculate one XPE per pair of measurement points. The specific error metrics utilized in Papers III and IV are based on the XPE values. These metrics were utilized in these research articles to facilitate the discussion of extrapolation errors when several reference and target points are evaluated simultaneously. For further technical details, the reader is referred to those articles.

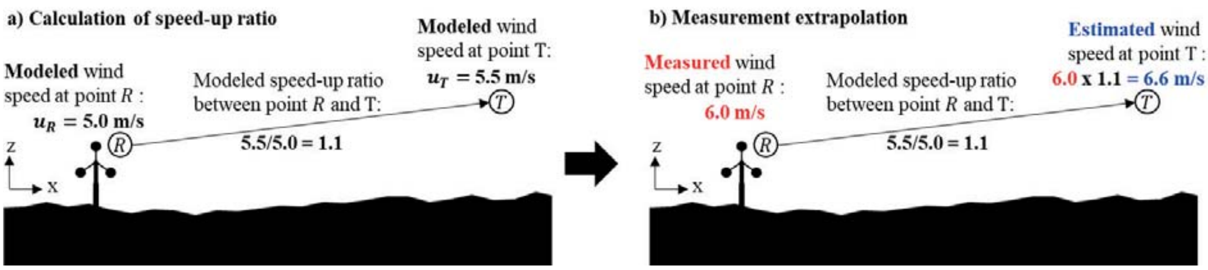

Figure 2.17. Example of the calculation of the speed-up ratio (a) and measurement extrapolation (b). Adapted from Paper I.

Summary of main results

In this chapter, the main results of this PhD thesis are presented. The findings can be ordered in three categories: (i) capabilities of the SOM2L classification, (ii) capabilities of coupled simulations and (iii) validation results of the meso-microscale coupling methodologies. Findings (i) focuses only in the strengths of the proposed classification, independent of the application. Findings (ii) and (iii) are related qualitatively and quantitatively results to the simulations of the coupled models.

3.1 Capabilities of the SOM2L classification

The SOM2L methodology proposed in Paper II provides in a fully automated manner the predominant patterns in the input data. In Paper II, the methodology was capable of finding wind speed profiles of various shapes. Some of these shapes correspond to well-known profiles, such as high shear, low shear or low-level jets. It was found that some of the obtained profiles had similar shape as the ones manually obtained in a observational study by Peña et al. (2014)[38], as shown in Figure 3.1. It is clear that the use of the SOM2L approach can be a better alternative to a more arduous manual approach.

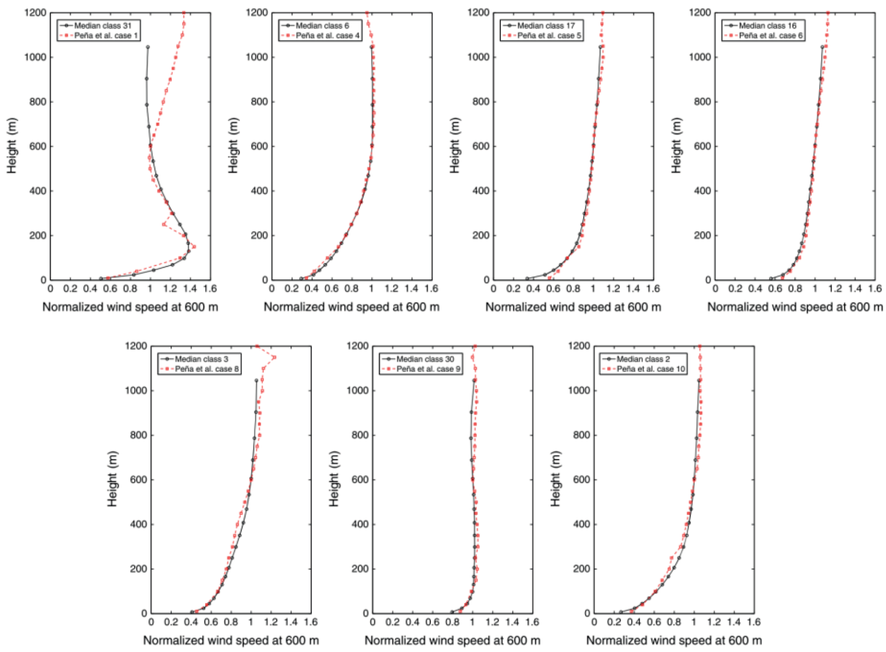

Figure 3.1. Comparison of a few wind speed vertical profiles reported by Peña et al. (2014)[38] against the SOM2L-based results. Reproduced from Paper II.

In Paper IV, the SOM2L is applied to the 3-D mesoscale fields simulated for the CK site. The SOM2L clearly provides distinctive patterns, regarding wind speed, wind direction and atmospheric stability. The methodology allows for an easy characterization of these patters. In particular for this site, relationships regarding wind direction, atmospheric stability, wind shear, time of the day and season were effortlessly explored due to the ordering provided by the SOM. Furthermore, a total number of 14 patterns were found, which is adequate for the computational resources typically available in the industry for downscaling purposes.

3.2 Capabilities of coupled simulations to downscale mesoscale patterns

Mesoscale models can reproduce some wind patterns that are not possible to obtain when utilizing a standalone microscale model. For some of the representative mesoscale fields, the coupled models are capable to downscale such mesoscale patterns. As shown in Figure 3.2, the overall mesoscale pattern is sustained in the microscale domain. However, the wind flow is modified by the microscale model by including the influence of finer terrain features in the local wind flow. As discussed in Paper III, the microscale model includes the influence of the mesoscale model in a better way in complex terrain, when the thermal effects are considered.

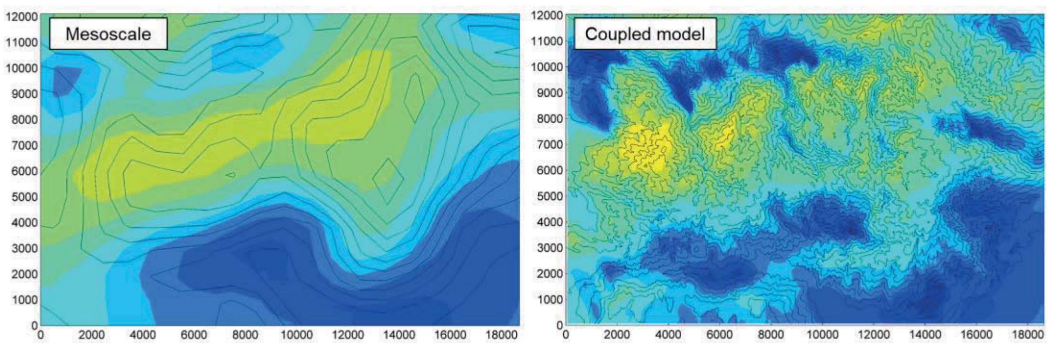

Figure 3.2. Horizontal planes of wind speed @ ~100 m from sector 150° at the CM site for mesoscale (left) and coupled (right) simulations. The black lines in the map correspond to the contour lines of terrain elevation for every 50 m. Adapted from Paper III.

Some wind patterns that are of interest for the wind energy community, namely strong wind turning and low-level jets, were reproduced by the WRF simulations. The coupled simulations are able to downscale these patterns into the microscale. As reported in Paper III, these patterns are very different from the ones obtained when using analytical profiles. In the case of the wind turning (Figure 3.3), the standalone microscale simulation does not present a turning at all. The same is true in the case of the low-level jets (Figure 3.4), as analytical formulations follow logarithmic shapes. For both patterns it was found that the use of atmospheric stability is necessary to maintain the wind turning and the low-level jet shape.

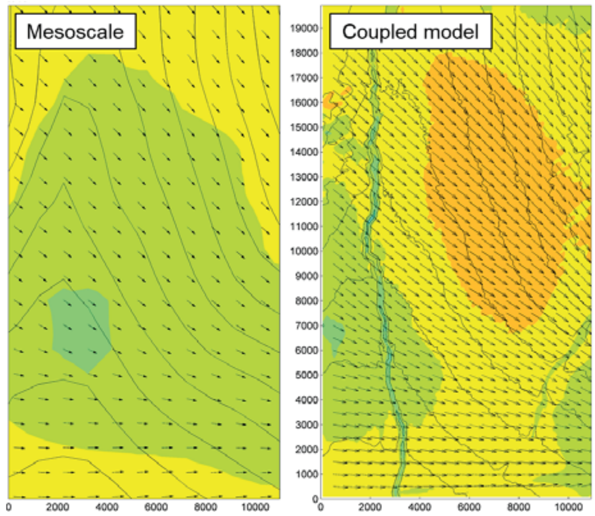

Figure 3.3. Horizontal planes of wind speed @ ~100 m from sector 300° at the CK site for mesoscale (left) and coupled (right) simulations. The black arrows indicate the direction of the wind. The black lines in the map correspond to the contour lines of terrain elevation for every 50 m. Adapted from Paper III.

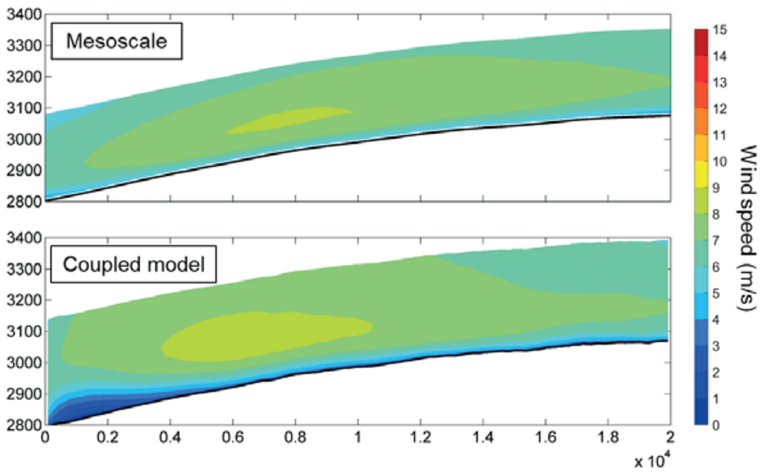

Figure 3.4. Vertical planes of wind speed from sector 0° at the CK site for mesoscale (left) and coupled (right) simulations. The black line corresponds to the digital terrain height. Adapted from Paper III.

3.3 Validation results

In this section the meso-microscale coupling results are evaluated. As mentioned in Section 1.1, the wind flow models are utilized to extrapolate onsite measurements. Therefore, the performance of the models is compared with respect to their capability to accurately do such extrapolations. The comparisons are conducted by using the crosscheck prediction errors explained in Section 2.4. This error metric is obtained by extrapolating a measurement to the location of another measurement and comparing the prediction against the observed values.

Further technical details of the meso-microscale coupling results using the mesoscale fields obtained from the directional average and from the SOM2L, can be found in the Papers III and IV, respectively.

3.3.1 Meso-microscale coupling using directional average

In Figure 3.5, the coupled models that utilize the directionally averaged mesoscale fields are compared against the mesoscale and the standalone microscale simulations. For vertical extrapolations, the coupled simulations have for most sectors smaller errors than the mesoscale or standalone simulations. Improvements of the coupled results respect to the mesoscale results, are mainly due to a better accounting of the influence of the finer features in the terrain. This is more evidently when comparing the results of the CM site, which is very complex. Moreover, in CA, where the terrain is very flat, the differences are rather small and actually mesoscale simulations perform slightly better as the wind profile is mostly influenced by the weather conditions rather than the terrain. Differences between coupled and standalone simulations are in general lower, as the latter uses analytical profiles whose parameters were adapted to the observed profiles. Nevertheless, there are important differences in the performance at some sectors. The source of these differences is the limitation of the analytical boundary conditions to reproduce non-analytical shapes. For example, very stable conditions present at CA were, as expected, associated with very high wind shear. This shear is well reproduced in the standalone simulation close to the ground. Nevertheless, it fails in reproducing very fast vertical changes of shear that are observed at the site as they do not follow an analytical shape. In the case of the CL site, very low shear profiles are observed due to the presence of wide low-level jets that are not possible to capture in the standalone simulations.

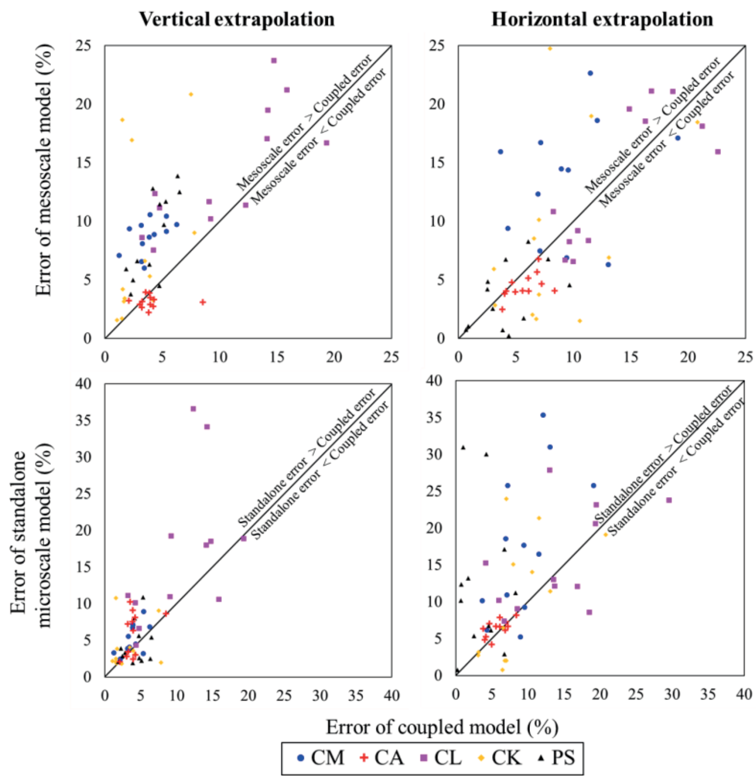

Figure 3.5. Comparison of crosscheck prediction errors between the mesoscale and coupled simulations (top panels), and standalone and coupled simulations (bottom panels). Adapted from Paper III.

For horizontal extrapolations in complex terrain (e.g. CM site), the coupled model performs better than the mesoscale and standalone simulations. This indicates that to properly model such sites it is not only sufficient to utilize models with finer resolution, but also with the adequate stability conditions. In the case of the very flat and very stable sites (e.g. CA site), it is better not to couple the potential temperature and run with neutral stratification instead. As discussed in Paper III, the inclusion of the atmospheric stability under these conditions results in too low turbulence in the microscale model to transfer the momentum downwards. At the remainder of the studied sites, the relative performance of the mesoscale and coupled simulations are very dependent on the wind direction. If the wind is perturbed by even smalls obstacles like small valleys, rivers, ridges or small hills, the coupled simulations tend to perform better. It must be noted that even when the mesoscale and coupled errors are similar, the latter have much finer features in the wind flow due to their higher resolution. Similar as with the vertical extrapolation, the coupled models perform better than the standalone simulation for most sectors, independent of the terrain or stability conditions. Depending on the sector, these differences are product of improver stability conditions in the standalone model (due to limited information) or due to the influence of mesoscale patterns that are significantly different to the analytical formulations.

3.3.2 Meso-microscale coupling using SOM2L patterns

Similar to the results in Section 3.3.1, most of the extracted patterns by the SOM2L are significantly modified by the microscale model. The main factors for these modifications are the finer terrain features included in the microscale model as well as the propagation of the wind conditions at the inlets into the domain. For most patterns with stable atmospheric conditions (patterns 1, 2, 4 and 8; see Figure 3.6), the microscale model reduces the error significantly, ranging from 4 to 15 % in error reduction (Figure 3.7). For most patterns with unstable atmospheric conditions (patterns 5, 9, 11 and 13) the microscale simulation performs worse than the mesoscale one, with an error increase between 3 to 7 %. A similar trend is observed for the neutral simulations, where the most stably stratified (pattern 12) has an error reduction of 2% and the most unstably stratified (patterns 6 and 10) have an error increase of 7% and 4% after downscaling, respectively. Overall, the error is reduced by 2.7% when using the downscaling procedure.

The mesoscale and microscale simulations of the SOM2L patterns produce very similar vertical profiles of wind speed. In addition, for most patterns both simulations reproduce well the measured winds speed profiles. For patterns with unstable atmospheric conditions (patterns 5, 9, 11, 13 and 14), the wind speeds profiles are particularly well reproduced. For patterns 4, 7 and 8, none of the models is able to reproduce the negative shear observed at the measurements. These deviations are due to the inability of the WRF model to reproduce the height of the jet for these patterns, a defect that is transferred to the microscale model. In the case of the pattern 3, the jet height is well reproduced and therefore is also correct in the microscale.

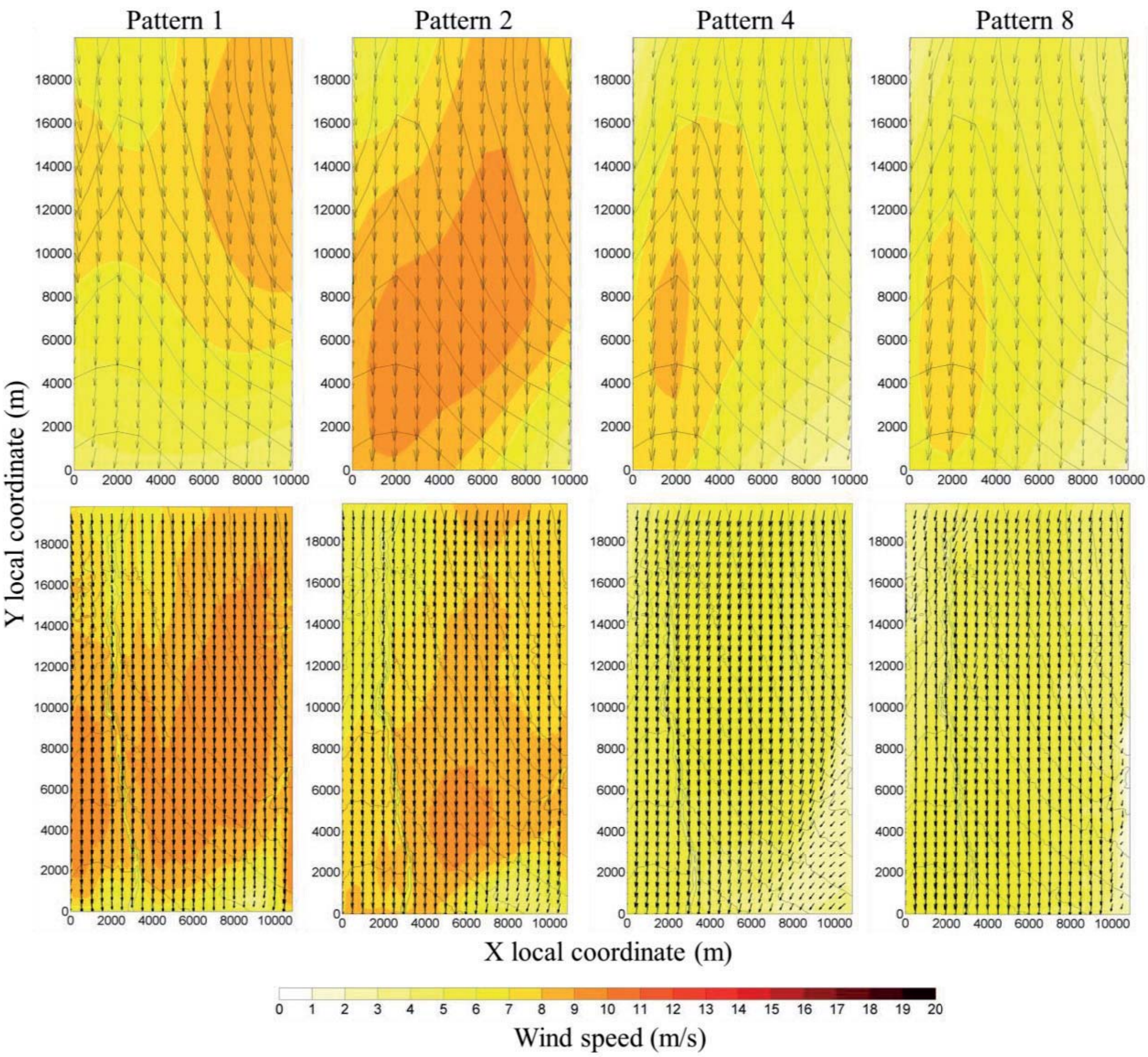

Figure 3.6. Extracted (top row) and downscaled (bottom row) patterns 1, 2, 4 and 8. The wind direction is indicated by the black arrows. Adapted from Paper IV.

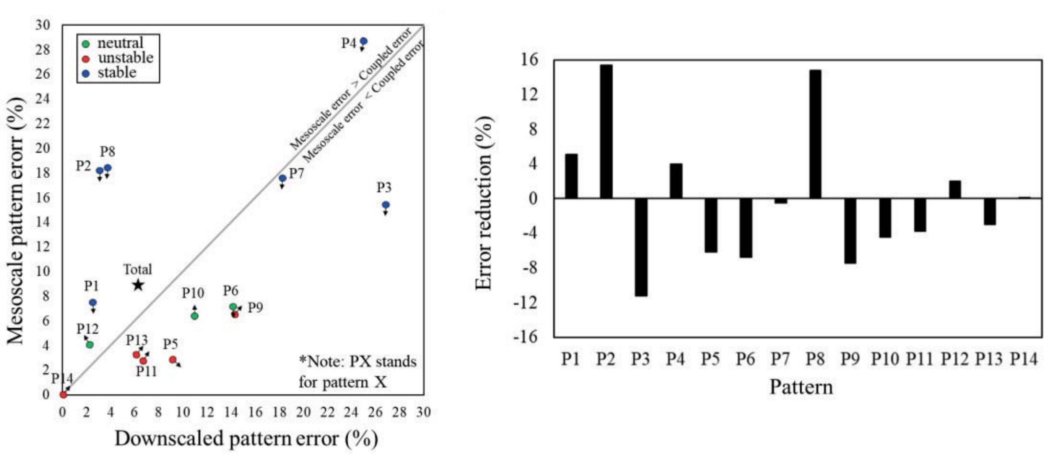

Figure 3.7. Left panel: Comparison of the crosscheck prediction errors between the mesoscale and downscaled patterns. The arrow and color of each circle indicate the wind direction and the atmospheric stability condition of the pattern, respectively. Right panel: Crosscheck prediction error reduction after downscaling the patterns. Reproduced from Paper IV.

Conclusions and further work

Two methodologies have been proposed for the coupling of mesoscale simulations with steady-state CFD microscale model. The first methodology utilizes the average values of the variables of interest per directional sector. Such a methodology is an easy way to produce more realistic boundary conditions for the microscale model. However, in some cases the averaged values of different weather conditions do not provide a good representation of the mean state of the atmosphere. The second proposed methodology derives predominant weather patterns utilizing a two-level self-organizing map clustering technique. This clustering technique fully automates the obtention of the mesoscale patterns and splits them according to their characteristics. Compared to the previous method, the loss of information is much lower as the averaging of values is conducted over similar mesoscale fields. This methodology is also able to deal with sites with different weather conditions despite of having similar wind directions.

Further remarks of the research conducted in this thesis are provided in the following paragraphs. In addition, recommendations for further research are provided for each topic.

4.1 Coupled models for wind resource assessment

Coupled simulations reproduce better the observed profiles compared to standalone simulations, if the shape of the profiles does not follow analytical formulations. Otherwise, the difference between the models is rather low. However, vertical validations in this study (and in general) are rarely conducted for heights higher than 150 m. For these heights, the coupled simulations present more realistic wind shear compared to the standalone simulations as the analytical formations (which are based on Monin-Obukhov similarity theory) are usually not valid anymore. This is important to consider in wind resource assessment as wind turbines get higher and higher. Coupled simulations tend to better reproduce the profiles at higher heights because of the information about the wind shear provided by the mesoscale model. However, the coupled models also perform better than the mesoscale model in vertical extrapolations because the latter are not able to properly take into account the influence of the surface on the lower part of the profiles.

For horizontal extrapolations, the use of coupled models performs better compared to mesoscale or standalone microscale models. In the case mesoscale models, the coupled models are simple more beneficial due to their higher resolution. In the case of microscale simulations, the coupled models have the advantage of a proper stability effects without the need of tweaking the stability conditions. Furthermore, make use of spatial distribution of the atmospheric stability in the site. This appears to be as important as using a finer resolution. which is of big importance for a proper modelling in complex terrain. Even if mesoscale simulations perform similar than the coupled model in terms of errors (typically at relatively flat terrain), the coupled model is able to include finer features in the wind flow, like rivers or forest clearings. This makes the coupled approach more advantageous for the micro-siting of the wind turbines.

For very stable conditions at flat sites, the coupled model is not capable to perform well in both vertical and horizontal extrapolations, simultaneously. Vertical extrapolations are better than any of the other models when thermal effects are considered. For horizontal extrapolations, the mesoscale and coupled models where similar, if in the latter neutral stratification is considered. When stable stratification is used instead, there is not sufficient turbulence in the microscale model to transfer momentum downwards. For very stable conditions, the wind has a quasi-laminar behavior, while turbulence models like the k-ε standard model are designed for turbulent flow. In order to enable the use of steady-state CFD models for meso-microscale coupling, it is recommended to further research modelling alternatives or modifications to RANS. This may include the addition of forcing terms based on observational data (nudging).

The validation study carried out through this work can be extended to other problems in wind resource assessment, like assessing the sensitivity of the energy yield and/or wind farm layout due to the use of mesoscale, standalone or coupled approaches. Moreover, it is recommended to further investigate and validate the turbulence intensity simulated by these set-ups. The turbulence intensity is key for site suitability studies of the wind turbines, which is important for wind energy project developers as well as for wind turbine manufacturers.

4.2 Two-level self-organizing map clustering methodology

The two-level self-organizing map technique proposed in this PhD thesis can in an objective manner extract the predominant wind patterns from a dataset. The methodology does not require any a priori prescription of cluster size and prevents the use of excessively large number of clusters by reducing redundant classes. The self-organizing map allows for the analysis of how the extracted patterns evolve with respect to time and space, and therefore associate them with underlying atmospheric phenomena or processes. The SOM2L has a lot of potential for different applications in wind energy. Below, some possible applications are listed:

i. With use concepts from the field of symbolic dynamics, it would be possible to study the evolution of certain wind patterns. Predominant sequences of patterns can be then be identified to be downscaled

ii. Classification of onsite measurements to explore the different conditions monitored by the instruments

iii. The patterns extracted from measured or simulated datasets can be used as states in Markov chains (or similar) for data reconstruction or for the generation of a typical year

iv. Wind energy forecasting frameworks

The applications listed above are only tentative and they require further research to be properly implemented.

4.3 Potential of coupled models using SOM2L

For the studied site in Paper IV, the meso-microscale coupling framework utilizing SOM2L improves the wind estimations compared with the use of the mesoscale model. Nevertheless, the microscale model is not able to properly downscale some of the obtained wind conditions. The reason is that the microscale model is only able to provide information from the inlets into the domain. Therefore, any pattern that is located within the domain and not “seen” at the inlets is not kept in the microscale simulation. In general, the weather conditions at the studied site were rather extreme (from very stable to very unstable stratification). Further validation of the methodology is required for simpler weather conditions as well as for more complex terrain.

Assuming that it is possible to properly downscale the extracted patterns by the SOM2L, the proposed framework has a lot of potential for wind turbine wake simulations. In order to resolve the turbine wake in a steady-state CFD model, different wind speeds for the same wind direction must be simulated. This increase the number of total simulations dramatically, even more if different atmospheric stability classes must be taken into account. With the SOM2L, infrequent combinations can be skipped, and only simulate the predominant ones.

References

1. Intergovernmental Panel on Climate Change. *Climate Change 2014 Mitigation of Climate Change*. (Cambridge University Press, 2014). doi:10.1017/CBO9781107415416.
2. GWEC. Global Wind Report 2015. 75 (2016).
3. Stehly, T., Beiter, P., Heimiller, D. & Scott, G. *2017 Cost of Wind Energy Review*. (2018).
4. Jackson, P. S. & Hunt, J. C. R. Turbulent wind flow over a low hill. *Q. J. R. Meteorol. Soc.* **101**, 929–955 (1975).
5. Yamaguchi, A., Ishihara, T. & Fujino, Y. Applicability of Linear and Nonlinear Winnd Prediction Models To Wind Flow in Complex Terrain. in *The World Wind Energy Conference and Exhibition* (2002).
6. Sanz Rodrigo, J. *et al.* Mesoscale to microscale wind farm flow modeling and evaluation. *Wiley Interdiscip. Rev. Energy Environ.* **6**, (2017).
7. Hristov, Y., Oxley, G. & Žagar, M. Improvement of AEP Predictions Using Diurnal CFD Modelling with Site-Specific Stability Weightings Provided from Mesoscale Simulation. *J. Phys. Conf. Ser.* **524**, 012116 (2014).
8. Monin, A. S. & Obukhov, A. M. Basic laws of turbulent mixing in the surface layer of the atmosphere. *Contrib. Geophys. Inst. Acad. Sci. USSR* **24**, 163–187 (1954).
9. New European Wind Atlas. www.neweuropeanwindatlas.eu.
10. Dutch Offshore Wind Atlas. https://www.dutchoffshorewindatlas.nl/.
11. Jothiprakasam, V. D. Downscaling wind energy resource from mesocale to local scale by nesting and data assimilation with a CFD model. 183 (2014).
12. Farr, T. G. *et al.* The Shuttle Radar Topography Mission. *Rev. Geophys.* **45**, RG2004 (2007).
13. Canadian Digital Elevation Model. https://open.canada.ca/data/en/dataset/7f245e4d-76c2-4caa-951a-45d1d2051333.
14. National Land Survey of Finland. https://www.maanmittauslaitos.fi/en.
15. Jun, C., Ban, Y. & Li, S. Open access to Earth land-cover map. *Nature* **514**, 434–434 (2014).
16. Wickham, J. *et al.* The Multi-Resolution Land Characteristics (MRLC) Consortium — 20 Years of Development and Integration of USA National Land Cover Data. *Remote Sens.* **6**, 7424–7441 (2014).

17. Davenport, A. Rationale for determining design wind velocities. *Trans. Am. Soc. Civ. Eng.* **126**, (1960).
18. Skamarock, W. C. *et al.* A Description of the Advanced Research WRF Version 3. *Tech. Rep.* 113 (2008) doi:10.5065/D6DZ069T.
19. High Performance Computing Center North. https://www.hpc2n.umu.se/.
20. Vortex webpage. https://vortexfdc.com/.
21. Reynolds, O. On the Dynamical Theory of Incompressible Viscous Fluids and the Determination of the Criterion. *Philos. Trans. R. Soc. A Math. Phys. Eng. Sci.* **186**, 123–164 (1895).
22. Launder, B. E. & Spalding, D. B. The numerical computation of turbulent flows. *Comput. Methods Appl. Mech. Eng.* **3**, 269–289 (1974).
23. Launder, B. E. & Spalding, D. B. The numerical computation of turbulent flows. *Comput. Methods Appl. Mech. Eng.* **3**, 269–289 (1974).
24. Duynkerke, P. G. Application of the E – ϵ Turbulence Closure Model to the Neutral and Stable Atmospheric Boundary Layer. *J. Atmos. Sci.* **45**, 865–880 (1988).
25. Duynkerke, P. G. & Driedonks, A. G. M. A Model for the Turbulent Structure of the Stratocumulus–Topped Atmospheric Boundary Layer. *J. Atmos. Sci.* **44**, 43–64 (1987).
26. Green, S. R. Modelling Turbulent Air Flow in a Stand of Widely-Spaced Trees. *PHOENICS J. Comput. Fluid Dyn. its Appl.* 294–312 (1992).
27. Sanz, C. A Note on k - ε Modelling of Vegetation Canopy Air-Flows. *Boundary-Layer Meteorol.* **108**, 191–197 (2003).
28. Zhong, S. & Takle, E. S. An Observational Study of Sea- and Land-Breeze Circulation in an Area of Complex Coastal Heating. *J. Appl. Meteorol.* **31**, 1426–1438 (1992).
29. Goldreich, Y., Druyan, L. M. & Berger, H. The interaction of valley/mountain winds with A diurnally veering sea/land breeze. *J. Climatol.* **6**, 551–561 (1986).
30. Kohonen, T. K. *Self-Organizing Maps*. (Springer-Verlag, 2001).
31. Wu, S. & Chow, T. W. S. Clustering of the self-organizing map using a clustering validity index based on inter-cluster and intra-cluster density. *Pattern Recognit.* **37**, 175–188 (2004).
32. Vesanto, J. & Alhoniemi, E. Clustering of the self-organizing map. *IEEE Trans. Neural Networks* **11**, 586–600 (2000).
33. Vesanto, J. & Sulkava, M. Distance Matrix Based Clustering of the Self-Organizing Map. in *International Conference on Artificial Neural Networks 2002* 951–956 (Springer, Berlin, Heidelberg, 2002). doi:10.1007/3-540-46084-5_154.

34. Everitt, B. S., Landau, S., Leese, M. & Stahl, D. *Cluster Analysis*. (2011).
35. Arya, S. P. *Introduction to Micrometeorology*. (Academic Press, 1998).
36. Berkowicz, R. & Prahm, L. P. Evaluation of the profile method for estimation of surface fluxes of momentum and heat. *Atmos. Environ.* **16**, 2809–2819 (1982).
37. Han, J., Arya, S. P., Shen, S. & Lin, Y.-L. *An Estimation and Energy Atmospheric Theory of Turbulent Dissipation Boundary Kinetic Energy Rate Based on Layer Similarity. NASA technical report*. (2000).
38. Peña, A., Floors, R. & Gryning, S. E. The Høvsøre Tall Wind-Profile Experiment: A Description of Wind Profile Observations in the Atmospheric Boundary Layer. *Boundary-Layer Meteorol.* **150**, 69–89 (2014).

Paper I
Durán, P., Meißner, C., Rutledge, K., Fonseca, R., Martin-Torres, J. & Adaramola, M.S. 2019. Meso-microscale coupling for wind resource assessment using averaged atmospheric stability conditions. - Meteorologische Zeitschrift 28: 273-291.
DOI: 10.1127/metz/2019/0937

Paper II
Durán, P., Basu, S., Meißner, C. & Adaramola, M.S. 2019. Automated classification of simulated wind field patterns from multiphysics ensemble forecasts. - Wind Energy 23: 898-914.
DOI: 10.1002/we.2462

Paper III
Durán, P., Meiβner, C. & Casso, P. A new meso-microscale coupled modelling framework for wind resource assessment: A validation study. - Renewable Energy. (Submitted)

Paper IV
Durán, P. Wind resource assessment using a novel meso-microscale coupling framework based on two-level self-organized maps clustering: A preliminary study. (Manuscript)

ISBN: 978-82-575-1693-2
ISSN: 1894-6402

Norwegian University
of Life Sciences

Postboks 5003
NO-1432 Ås, Norway
+47 67 23 00 00
www.nmbu.no

106866 / ANDVORDGRAFISK.NO